EVALUATING THE ROLE OF SYNTHETIC MAGNETIC RESONANCE IMAGING (MRI) IN DIFFERENTIATING ACTIVE AND CHRONIC MULTIPLE SCLEROSIS (MS) PLAQUES ON THE BASIS OF QUANTITATIVE PARAMETERS NAMELY T1 RELAXATION RATE (R1), T2 RELAXATION RATE (R2), PROTON DENSITY (PD) AND MYELIN WATER FRACTION (MWF)

DR SACHIN GIRDHAR

DM NEURORADIOLOGY/INTERVENTIONAL RADIOLOGY THESIS

2022

SREE CHITRA TIRUNAL INSTITUTE FOR MEDICAL SCIENCES AND

TECHNOLOGY, TRIVANDRUM

An Institution of National Importance established by an Act of the Indian Parliament
(Act No.52 of 1980)
Dept. of Science and Technology, Govt. of India
www.sctimst.ac.in

EVALUATING THE ROLE OF SYNTHETIC MAGNETIC RESONANCE IMAGING (MRI) IN DIFFERENTIATING ACTIVE AND CHRONIC MULTIPLE SCLEROSIS (MS) PLAQUES ON THE BASIS OF QUANTITATIVE PARAMETERS NAMELY T1 RELAXATION RATE (R1), T2 RELAXATION RATE (R2), PROTON DENSITY (PD) AND MYELIN WATER FRACTION (MWF)

A THESIS SUBMITTED BY

DR SACHIN GIRDHAR

TO

SREE CHITRA TIRUNAL INSTITUTE FOR MEDICAL SCIENCES AND TECHNOLOGY, TRIVANDRUM.

IN PARTIAL FULFILMENT OF THE REQUIREMENTS

FOR THE AWARD OF

DM NEURORADIOLOGY/INTERVENTIONAL RADIOLOGY

2022

DECLARATION BY THE STUDENT

CERTIFICATE

I, **DR SACHIN GIRDHAR**, hereby certify that I had personally carried out the work depicted in the thesis titled, "**EVALUATING THE ROLE OF SYNTHETIC MAGNETIC RESONANCE IMAGING (MRI) IN DIFFERENTIATING ACTIVE AND CHRONIC MULTIPLE SCLEROSIS (MS) PLAQUES ON THE BASIS OF QUANTITATIVE PARAMETERS NAMELY T1 RELAXATION RATE (R1), T2 RELAXATION RATE (R2), PROTON DENSITY (PD) AND MYELIN WATER FRACTION (MWF)**".

No part of this thesis has been submitted for the award of any other degree or diploma prior to this date.

Signature

Name of the Candidate
Dr Sachin Girdhar

Date 11/08/2022

(* If external help was sought, declare and acknowledge)

श्री चित्रा तिरुनाल आयुर्विज्ञान और प्रौद्योगिकी संस्थान, त्रिवेन्द्रम
तिरुवनन्तपुरम - ६९५०११, केरल, इंडिया
SREE CHITRA TIRUNAL INSTITUTE FOR MEDICAL SCIENCES AND TECHNOLOGY, TRIVANDRUM
Thiruvananthapuram - 695 011, Kerala, India
(An Institute of National Importance under Govt. of India)
Grams : Chitramet, Phone : +91-471-2443152, Fax : +91-471-2550728 / 2446433, E-mail : sct@sctimst.ac.in, Website : www.sctimst.ac.in

CERTIFICATE BY THE RESEARCH GUIDE
(*in institute letterhead)

Name of the Guide: **Dr Bejoy Thomas, Prof & HOD**

Division/Department: **Dept of Imaging Sciences & Interventional Radiology**

This is to certify that **Dr Sachin Girdhar**, department of **Imaging Sciences & Interventional Radiology** of this institute has fulfilled the requirements prescribed for the **DM Neuroradiology/Interventional Radiology** degree of the **Sree Chitra Tirunal Institute for Medical Sciences and Technology, Trivandrum**.

The thesis entitled, "**EVALUATING THE ROLE OF SYNTHETIC MAGNETIC RESONANCE IMAGING (MRI) IN DIFFERENTIATING ACTIVE AND CHRONIC MULTIPLE SCLEROSIS (MS) PLAQUES ON THE BASIS OF QUANTITATIVE PARAMETERS NAMELY T1 RELAXATION RATE (R1), T2 RELAXATION RATE (R2), PROTON DENSITY (PD) AND MYELIN WATER FRACTION (MWF)**" was carried out under my direct supervision. No part of the thesis was submitted for the award of any degree or diploma prior to this date.

*Clearance was obtained from the Institutional Ethics Committee / Institutional Animal Ethics / Institutional Committee for Stem Cell Research / Other appropriate committees (if any, specify) for carrying out the study.

Signature

Dr. Bejoy Thomas

Name of the Guide

Date 11/8/2022

*As and when applicable. If an external co-guide was present, a similar declaration should be made, provided a substantial part of the thesis work was done under co-guide.

श्री चित्रा तिरुनाल आयुर्विज्ञान और प्रौद्योगिकी संस्थान, त्रिवेन्द्रम
तिरुवनन्तपुरम - ६९५०११, केरल, इंडिया
SREE CHITRA TIRUNAL INSTITUTE FOR MEDICAL SCIENCES AND TECHNOLOGY, TRIVANDRUM
Thiruvananthapuram - 695 011, Kerala, India
(An Institute of National Importance under Govt. of India)
Grams : Chitramet, Phone : +91-471-2443152, Fax : +91-471-2550728 / 2446433, E-mail : sct@sctimst.ac.in, Website : www.sctimst.ac.in

CERTIFICATE BY THE RESEARCH CO-GUIDE
(*in institute letterhead)

Name of the Co-Guide: **Dr C Kesavadas, Prof**

Division/Department: **Dept of Imaging Sciences & Interventional Radiology**

This is to certify that **Dr Sachin Girdhar**, department of **Imaging Sciences & Interventional Radiology** of this institute has fulfilled the requirements prescribed for the **DM Neuroradiology/Interventional Radiology** degree of the **Sree Chitra Tirunal Institute for Medical Sciences and Technology, Trivandrum**.

The work under the thesis entitled, "**EVALUATING THE ROLE OF SYNTHETIC MAGNETIC RESONANCE IMAGING (MRI) IN DIFFERENTIATING ACTIVE AND CHRONIC MULTIPLE SCLEROSIS (MS) PLAQUES ON THE BASIS OF QUANTITATIVE PARAMETERS NAMELY T1 RELAXATION RATE (R1), T2 RELAXATION RATE (R2), PROTON DENSITY (PD) AND MYELIN WATER FRACTION (MWF)**" was carried out under my direct supervision. No part of the thesis was submitted for the award of any degree or diploma prior to this date.

*Clearance was obtained from the Institutional Ethics Committee / Institutional Animal Ethics / Institutional Committee for Stem Cell Research / Other appropriate committees (if any, specify) for carrying out the study.

Signature 

Name of the Co-guide

Date 12/08/2022

Dr C. Kesavadas

Thesis generated from affiliated institutes shall use their letterhead. The letter should have line "MD/DM/MCh program affiliated to the Sree Chitra Tirunal Institute for Medical Sciences and Technology, Trivandrum)"

श्री चित्रा तिरुनाल आयुर्विज्ञान और प्रौद्योगिकी संस्थान, त्रिवेन्द्रम
तिरुवनन्तपुरम - ६९५०११, केरल, इंडिया
SREE CHITRA TIRUNAL INSTITUTE FOR MEDICAL SCIENCES AND TECHNOLOGY, TRIVANDRUM
Thiruvananthapuram - 695 011, Kerala, India
(An Institute of National Importance under Govt. of India)
Grams : Chitramet, Phone : +91-471-2443152, Fax : +91-471-2550728 / 2446433, E-mail : sct@sctimst.ac.in, Website : www.sctimst.ac.in

CERTIFICATE BY THE RESEARCH CO-GUIDE
(*in institute letterhead)

Name of the Co-Guide: **Dr Sruthi Nair, Associate Professor**

Division/Department: **Department of Neurology**

This is to certify that **Dr Sachin Girdhar**, department of **Imaging Sciences & Interventional Radiology** of this institute has fulfilled the requirements prescribed for the **DM Neuroradiology/Interventional Radiology** degree of the **Sree Chitra Tirunal Institute for Medical Sciences and Technology, Trivandrum**.

The work under the thesis entitled, "**EVALUATING THE ROLE OF SYNTHETIC MAGNETIC RESONANCE IMAGING (MRI) IN DIFFERENTIATING ACTIVE AND CHRONIC MULTIPLE SCLEROSIS (MS) PLAQUES ON THE BASIS OF QUANTITATIVE PARAMETERS NAMELY T1 RELAXATION RATE (R1), T2 RELAXATION RATE (R2), PROTON DENSITY (PD) AND MYELIN WATER FRACTION (MWF)**" was carried out under my direct supervision. No part of the thesis was submitted for the award of any degree or diploma prior to this date.

*Clearance was obtained from the Institutional Ethics Committee / Institutional Animal Ethics / Institutional Committee for Stem Cell Research / Other appropriate committees (if any, specify) for carrying out the study.

Signature 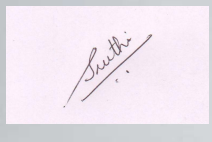

Name of the Co-guide
Dr Sruthi Nair

Date 12/08/2022

Thesis generated from affiliated institutes shall use their letterhead. The letter should have line "MD/DM/MCh program affiliated to the Sree Chitra Tirunal Institute for Medical Sciences and Technology, Trivandrum)"

श्री चित्रा तिरुनाल आयुर्विज्ञान और प्रौद्योगिकी संस्थान, त्रिवेन्द्रम
तिरुवनन्तपुरम - ६९५०११, केरल, इंडिया
SREE CHITRA TIRUNAL INSTITUTE FOR MEDICAL SCIENCES AND TECHNOLOGY, TRIVANDRUM
Thiruvananthapuram - 695 011, Kerala, India
(An Institute of National Importance under Govt. of India)
Grams : Chitramet, Phone : +91-471-2443152, Fax : +91-471-2550728 / 2446433, E-mail : sct@sctimst.ac.in, Website : www.sctimst.ac.in

APPROVAL OF THE THESIS

(*in institute letterhead)

The thesis entitled

Evaluating the role of Synthetic magnetic resonance imaging (MRI) in differentiating active and chronic multiple sclerosis (MS) plaques on the basis of quantitative parameters namely T1 relaxation rate (R1), T2 relaxation rate (T2), proton density (PD) and myelin water fraction (MWF)

Submitted by

Dr Sachin Girdhar

for the degree of

DM NEURORADIOLOGY/INTERVENTIONAL RADIOLOGY

of

SREE CHITRA TIRUNAL INSTITUTE FOR MEDICAL SCIENCES AND TECHNOLOGY, TRIVANDRUM

is evaluated and approved by

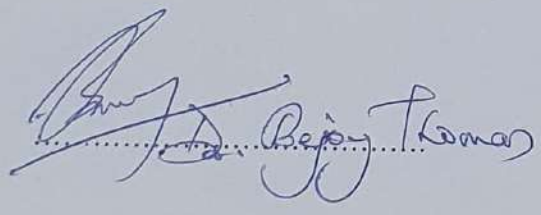

.....

(Name & Signature of the Guide)

(Name & Signature of thesis examiner)

ACKNOWLEDGEMENT

I am deeply indebted to my honorable teachers and guides Dr Bejoy Thomas and Dr C Kesavadas for their constant support, encouragement, helpful criticism, expert supervision and guidance throughout this study which assisted largely in bringing this study to fruition.

I am also thankful to Dr Sruthi Nair for her support and encouragement throughout the study.

I would specially like to acknowledge my gratitude to my past and present colleagues for their valuable guidance & constant support.

I would also like to extend my special gratitude to my family for being so supportive throughout my medical education years. I could not have come this far without their love and support.

Last but most important, I am grateful to all my patients & their relatives who have been the very basis of this study.

TABLE OF CONTENTS

LIST OF FIGURES

LIST OF TABLES

SYNOPSIS

EVALUATING THE ROLE OF SYNTHETIC MAGNETIC RESONANCE IMAGING (MRI) IN DIFFERENTIATING ACTIVE AND CHRONIC MULTIPLE SCLEROSIS (MS) PLAQUES ON THE BASIS OF QUANTITATIVE PARAMETERS NAMELY T1 RELAXATION RATE (R1), T2 RELAXATION RATE (R2), PROTON DENSITY (PD) AND MYELIN WATER FRACTION (MWF)

SYNOPSIS

BY

DR SACHIN GIRDHAR

for DM NEURORADIOLOGY/INTERVENTIONAL RADIOLOGY Degree

of

SREE CHITRA TIRUNAL INSTITUTE FOR MEDICAL SCIENCES AND TECHNOLOGY, TRIVANDRUM

(The typed pages may be stapled and submitted three months prior to the submission of the thesis. When synopsis forms part of the thesis, the cover page need not be included)

SYNOPSIS

Background and purpose: Contrast MRI forms the mainstay for imaging evaluation of multiple sclerosis patients not only for diagnosis and ruling out other differentials, but also for monitoring disease activity and therapeutic monitoring. Repeated usage of gadolinium contrast not only adds to scan cost and duration but also poses risk of adverse events. The aim of current study was to explore the utility of novel synthetic MRI-derived quantitative parameters in identifying active multiple sclerosis lesions without injecting contrast.

Materials and Methods: Forty three clinically suspected or confirmed MS patients underwent conventional contrast MRI examinations along with a synthetic MRI sequence. ROIs were placed on synthetic FLAIR images in MS lesions (enhancing and non-enhancing) and quantitative parameters of R1, R2, PD and MyC obtained. Statistical analysis of these quantitative values was performed by receiver operating characteristic (ROC) analysis and logistic regression analysis.

Results: Contrast enhancing MS lesions demonstrated significantly higher mean R1, R2 and lower mean PD values in comparison to non-enhancing MS lesions.

Conclusion: Synthetic MRI derived quantitative parameters of R1, R2 and PD can be used to differentiate contrast enhancing from non-enhancing MS lesions without giving gadolinium contrast.

1 Introduction

Multiple sclerosis is the commonest primary demyelinating disease largely afflicting young, professionally active population and encompasses complex, immune-mediated neuropathological processes including varying degrees of inflammation, oedema, astrogliosis, neurodegeneration and axonal loss, myelin breakdown, and remyelination (1). In addition to focal demyelinated plaques, diffuse global damage is also noted in normal appearing brain tissue, as delineated by advanced MR techniques like MR spectroscopy and DTI (2,3).

Conventional MRI with gadolinium based contrast agent (CE-MRI) forms a major component of the diagnostic armamentarium available to present day clinicians in evaluating MS patients. CE-MRI enables detection of active plaques (post contrast enhancement ascribed to active blood-brain barrier breakdown) and chronic plaques (non-enhancing). This helps not only in diagnosis of multiple sclerosis as per McDonald's criteria of dissemination in time but also in eliminating important differential diagnoses (4). Further, contrast-enhanced MRI is also used in follow-up of multiple sclerosis patients for diagnosing complications (opportunistic infections like progressive multifocal leucoencephalopathy), detecting relapses (multiple acute, enhancing lesions), monitoring therapy and prognosticating chronic long term sequelae (brain atrophy).

Repeated usage of gadolinium based contrast agent in multiple sclerosis diagnosis and evaluation not only exposes the patients to risk of nephrogenic systemic fibrosis (NSF), especially with renal insufficiency but also adds significantly to the cost as well as duration of the study (5,6). An effective imaging modality with high precision for MS plaque evaluation and characterisation without any need of contrast agent administration will significantly help mitigate the contrast related risks enumerated earlier.

Synthetic MRI is a novel MR protocol that is not only super-fast (scan time less than 6 min; post processing less than 1 minute) but also allows parametric quantification of tissue-

related, inherent physical properties that determine signal characteristics on conventional MR images – proton density (PD) and T1/T2 relaxation rates (7–10).This accurate method of tissue relaxometry enables synthesis of user-defined contrast-weighted MR images, non-user dependent brain segmentation as well as myelin volume estimation based on obtained quantitative parameters (6–15)(7,9,11).

Based on different ongoing neuropathological processes in acute vis-a-vis chronic plaques, it is proposed that synthetic MRI derived absolute, quantitative parameters may help distinguish acute from chronic MS plaques. If positively established, use of synthetic MRI for MS evaluation may not only lead to fast imaging times, less operator dependence and zero patient recalling but also obviate the need of administering gadolinium based contrast agent for depicting active disease.

AIMS AND OBJECTIVES

1. Evaluating the role of quantitative parameters derived from synthetic magnetic resonance imaging (MRI) derived quantitative parameters namely T1 and T2 relaxation rates (R1 and R2 respectively) and proton density (PD) values in differentiating active from chronic multiple sclerosis (MS) plaques.
2. Exploring the utility of synthetic MRI derived myelin correlated volume values in identifying active multiple sclerosis (MS) plaques.

2 LITERATURE REVIEW

Introduction

Multiple sclerosis is the most commonly encountered primary demyelination disorder with significant neurological morbidity afflicting young adult population other than trauma in the prime of their life. While it was commonly described in developed nations at higher latitudes, this view no longer holds true as more and more cases are being diagnosed in tropical countries like India. It is a heterogeneous disease caused by complex interplay between genetic predispositions and a host of environmental factors. The clinical course varies from the most common relapsing remitting pattern to progressive patterns like secondary and primary progressive multiple sclerosis (SPMS and PPMS respectively). The most widely held view describes the disease process in 2 stages-recurrent neuroinflammation presenting as relapsing remitting multiple sclerosis (RRMS) and accumulating neurodegeneration causing early or gradual disease progression to more aggressive forms of multiple sclerosis. Recent introduction of promising pharmacology regimes in the form of highly effective disease altering therapies are changing the landscape of multiple sclerosis management at a fast pace (12).

Epidemiology and Risk Factors

Multiple sclerosis most commonly afflicts young adult population. The mean age of onset ranges from 25 to 40 years in different studies. Although its incidence has been found at either extremes of age - children less than 10 years of age to older adults more than 50 years of age, such a presentation is extremely rare (13). An earlier age of onset (mean 25-29 years) is generally observed in relapsing remitting multiple sclerosis (RRMS) in comparison to secondary and primary progressive multiple sclerosis.

It is commonly believed that multiple sclerosis affects females more commonly than males. A systematic review of more than 25 studies discovered that there has been an increasing trend of female preponderance in multiple sclerosis over the recent years compared to earlier literature (14).

Being an autoimmune condition, several studies have concluded that multiple sclerosis may have an association with other autoimmune disorders. Recent meta-analysis published in 2015 concluded that psoriasis and thyroid disease are the most prevalent autoimmune conditions associated with multiple sclerosis (less than 10%). Also, patients with multiple sclerosis may have a slightly higher risk of developing uveitis and inflammatory bowel disease compared to the general population (15).

Several genetic studies have elucidated prominent genetic associations in relation to multiple sclerosis (16). Genomic association studies have implicated around 200 polymorphisms attributed with risk of developing multiple sclerosis. Further, a particularly strong association has been noted with alleles of major histocompatibility complex (MHC) in HLA-DRB1 locus. Other less common associations are with numerous genes like CD 6, CLEC16A, IL7R and IRF8 (17).

A multitude of environmental factors have also been postulated in the pathogenesis of multiple sclerosis. EBV (Epstein Barr Virus) is widely considered as one of the foremost environmental factors predisposing to multiple sclerosis. Although several studies have found an association between the two, conclusive evidence is difficult to establish in view of high prevalence of Epstein Barr virus even in normal, healthy population (18–20).

A multitude of studies have found that increased exposure to sunlight and ultraviolet radiation has a protective effect against multiple sclerosis, possibly explaining higher

prevalence of multiple sclerosis at higher latitudes (21–23). Also, reduced serum Vitamin D levels that may be associated with genetic variation or diminished sunlight exposure, may aggravate the susceptibility to multiple sclerosis (22).

Other environmental triggers implicated in the pathogenesis of multiple sclerosis include tobacco smoking (24), childhood or adolescent obesity (25) and altered gut microbiome (26).

Clinical presentation and disease pattern

Multiple sclerosis has been categorised into following subtypes depending on the clinical presentation:

1. Relapsing remitting multiple sclerosis (RRMS)

2. Clinically isolated syndrome (CIS)

3. Secondary progressive MS (SPMS)

4. Primary progressive MS (PPMS)

Clinical manifestations of multiple sclerosis are nonspecific and most commonly include sensory disturbances in limbs or one side of face, visual diminution in one eye, subacute muscle weakness, double vision, gait imbalance, shock like sensation along the spine during neck flexion (Lhermitte's phenomenon) and giddiness. Pain is not a common initial presentation of multiple sclerosis and has been reported in less than 20% of cases. Patients often complain of more than one temporal episodes of neurological dysfunction at the time of initial presentation with complete or at least some recovery.

Relapsing remitting multiple sclerosis (RRMS) is the most commonly encountered clinical subtype seen in around 85 to 90% of MS cases. Relapsing remitting multiple sclerosis is characterised by clinically discrete attacks of neurological dysfunction with full or near complete recovery between attacks. Clinical along with radiological dissemination in time and space (as determined by new T2/FLAIR hyperintense or contrast enhancing lesions on MRI) forms the cornerstone for confirming diagnosis of relapsing remitting multiple sclerosis.

Clinically isolated syndrome (CIS) is usually defined as initial or first presentation of neurological dysfunction that may precede multiple sclerosis and that may develop acutely or subacutely.

10 to 15% of patients may show progressive neurological dysfunction without intervening episodes of remission, that is labelled as primary progressive MS. It is characterised by progressive neurodegeneration and consequent evolving disability right from the time of disease onset with transient intervening minor improvements only.\

Secondary progressive MS is characterised by a disease course that resembles typical relapsing remitting multiple sclerosis initially followed by slow clinical worsening. This transition usually happens 15 to 20 years after disease onset.

Diagnostic Evaluation

Detailed history and clinical examination cannot be overemphasised in the initial evaluation of suspected central nervous system (CNS) demyelination disorder. Specifically, history should include details of any prior episodes with neurological symptoms that are characteristic of inflammatory demyelination.

Contrast MRI evaluation of brain and spinal cord is of paramount importance in initial diagnostic evaluation of suspected MS especially so in patients presenting with atypical clinical presentation and for ruling out close differentials such as MOGAD (myelin oligodendrocyte glycoprotein antibody-associated disease), NMOSD (neuromyelitis optica spectrum disorders) and central nervous system (CNS) vasculitis.

As per the 2017 revised McDonald criteria (Table 1) (4) for multiple sclerosis diagnosis in patients having greater than two clinical attacks but objective clinical evidence of only one lesion stress upon the MR demonstration of dissemination in space as defined by characteristic T2 hyperintense lesion in at least two out of four characteristic sites (cortical / juxta-cortical, periventricular, infratentorial along with spinal cord) or an additional clinical attack supported by objective clinical evidence that involves a different central nervous system (CNS) site.

Similarly in patients with first clinical attack, also called clinically isolated syndrome (CIS), with imaging evidence of 2 or more lesions, McDonald criteria require additional evidence of dissemination in time as confirmed by development of a fresh neurological attack supported by objective clinical evidence **or** MR depiction of enhancing as well as non-enhancing lesions simultaneously at a given time **or** by demonstration of new enhancing or T2 hyperintense lesions on serial MRI imaging **or** by demonstration of oligoclonal bands in cerebrospinal fluid (CSF).

Radiologically isolated syndrome (RIS) is defined by absence of typical clinical manifestations of MS and presence of incidental brain or spinal cord MR findings highly suggestive of MS depending on the typical morphology and parenchymal location of the lesions. For patients with RIS who fulfill McDonald criteria for dissemination in space, MS diagnosis can be made if MRI evaluation establishes dissemination in time **AND** there is subsequent development of a new neurological event confirmed by objective clinical evidence.

It is important to understand that McDonald criteria are applicable only after optimal clinical evaluation and they have no significant value in isolation. The diagnosis of MS is entertained only if the criteria are fulfilled after excluding other causes for similar clinical or radiological presentation. The diagnosis of possible MS may be assumed if the patient has clinically isolated syndrome but fails to meet the McDonald criteria. MS diagnosis is considered highly unlikely if some other condition can be attributed to the clinical presentation.

	Number of lesions with objective clinical evidence	Additional data needed for a diagnosis of multiple sclerosis
≥2 clinical attacks	≥2	None*
	1 (as well as clear-cut historical evidence of a previous attack involving a lesion in a distinct anatomical location¶)	None*
	1	Dissemination in space demonstrated by an additional clinical attack implicating a different CNS site or by MRI$^{\Delta}$
1 clinical attack	≥2	Dissemination in time demonstrated by an additional clinical attack or by MRI$^{\diamond}$ **OR** demonstration of CSF-specific oligoclonal bands§
	1	Dissemination in space demonstrated by an additional clinical attack implicating a different CNS site or by MRI$^{\Delta}$ **AND** Dissemination in time demonstrated by an additional clinical attack or by MRI$^{\diamond}$ **OR** demonstration of CSF-specific oligoclonal bands§

Table 1: 2017 McDonald criteria for diagnosis of multiple sclerosis in patients with an attack at onset (4)

Differential Diagnoses

A multitude of inflammatory, infectious, genetic, granulomatous and other miscellaneous disorders (Table 2) should be considered when evaluating a suspected case of multiple sclerosis (MS). MS diagnosis becomes more difficult especially in cases with atypical clinical presentation, progressive course of illness, monophasic clinical episode, younger or older age of onset and absence of typical MRI findings.

Inflammatory Diseases
ADEM (Acute Disseminated Encephalomyelitis)
NMOSD (Neuromyelitis optica spectrum disorder)
MOGAD (Myelin oligodendrocyte glycoprotein antibody associated encephalomyelitis)
CLIPPERS (Chronic Lymphocytic Inflammation with pontine Perivascular Enhancement Responsive to Steroids)
Neuro-Behcets'
PAN (Polyarteritis nodosa)
PACNS (Primary Angiitis of Central Nervous System)
Sjogren Syndrome
Infections
Neurosyphilis
HIV
PML (Progressive Multifocal Leukoencephalopathy)
Lyme's Disease
Genetic Diseases
CADASIL (Cerebral autosomal dominant arteriopathy with subcortical infarcts and leukoencephalopathy)
Inflammatory and Granulomatous Diseases
Lymphomatoid Granulomatosis
Neurosarcoid
Wegener's
Myelin Disorders
Adrenoleukodystrophy (ALD)
Adult metachromatic leukodystrophy (MLD)

Table 2: Differential Diagnoses of multiple sclerosis

However, certain clinical features have been described that should raise the suspicion of alternate diagnosis. Red flag signs (4,27) that warranty consideration of other differential diagnosis include the following:

-Hyperacute presentation (Ischemic stroke, seizures)

-Leptomeningeal disease

-Encephalopathy (ADEM, PRES, MOGAD, Infectious & Auto-immune encephalitis)

-Progressive ataxia (SCA, paraneoplastic or auto-immune syndromes)

-Cognitive dysfunction (Neurodegenerative diseases, genetic leukoencephalopathies)

-Meningismus or headache (ADEM, CVT, Chronic meningitis, Vasculitis, SLE, Neoplasm)

-Dominant brainstem symptoms (Neuro-Behcet's, Neurosarcoid, CLIPPERS, TB)

-Simultaneous bilateral optic neuritis (NMOSD, MOGAD)

-Longitudinally extensive spinal cord lesion on MRI (NMOSD, MOGAD)

-Persistent back pain

-Rapidly progressive disease course

-Systemic symptoms such as weight loss, fever and night sweats (Infection, Vasculitis, SLE)

-Family history of other neurological diseases (CADASIL)

-Cortical features like aphasia or neglect syndrome

Magnetic Resonance Imaging (MRI)

As described above contrast MRI is the imaging procedure of foremost significance in initial diagnostic evaluation of multiple sclerosis. McDonald criteria for Ms require specific MR findings such as lesion dissemination in time and space for confident MS diagnosis (4). MRI has a high sensitivity and specificity up to 87 and 73% respectively for establishing dissemination in space as per McDonald criteria (28).

Lesion morphology

MS plaques are typically described as ovoid, T2/FLAIR hyperintense lesions in the typical locations of cortical/juxta-cortical region, periventricular white matter, corpus callosum including calloso-septal interface, infratentorial compartment, optic nerves and spinal cord. The periventricular lesions are oriented at right angles to the ventricular margin and are referred to as Dawson's fingers. A few lesions in chronic, longstanding MS may become hypointense on T1-weighted images and are labelled as black holes. Infratentorial involvement is most commonly noted involving pons, midbrain and cerebellar peduncles. Sub-pial distribution of T2 hyperintense plaques in the brainstem is a characteristic finding of MS. Advanced MR techniques like magnetic resonance spectroscopy (MRS) and diffusion tensor imaging (DTI) have also demonstrated contiguous involvement of NAWM (normal appearing white matter) in MS patients. As the disease progresses, neurodegeneration sets in and diffuse neuroparenchymal volume loss/atrophy is appreciated on MRI.

Spinal cord lesions

Spinal cord involvement in MS is relatively common and typically described as focal, eccentric, short segment (<2 vertebral length), T2 hyperintense lesions occupying less than half cord cross sectional area (29,30). Cervical cord is the most common site of predilection.

Optic nerve lesions

Optic nerve involvement in Ms is fairly common. Optic nerve lesions are usually focal, short segment, bilaterally asymmetric and usually involving anterior segments of the optic nerves.

Active versus chronic lesions

Acute MS lesions signify disease activity. They tend to be larger in size as compared to chronic lesions and have poorly defined margins. They characteristically show contrast enhancement that may be solid, peripheral or inhomogeneous and signifies blood brain barrier breakdown as part of inflammatory process. Contrast enhancement usually persists for an average duration of up to 3 weeks (31). Studies have shown that persistence of active enhancing lesions on serial MRI points towards a continuous disease activity (32,33).

Advanced MRI techniques

The conventional MRI is incapable of distinguishing the varied neuro-inflammatory processes of MS that include varying degrees of demyelination, remyelination, axonal loss and gliosis. Further, it cannot detect normal appearing white matter (NAWM) pathology that is actually abnormal in MS. MR spectroscopy is a quantitative imaging technique that generates quantitative information about chemical metabolites such as NAA (N-Acetyl Aspartate), creatine phosphate, choline containing compounds, lactic acid etc. Reduction of NAA or reduced NAA/Cr ratio has been described in patients with chronic MS, thereby implying neuronal loss and is a prognostic marker in assessing long term disability in MS (34). Diffusion

tensor imaging (DTI) enables assessment and delineation of fractional anisotropy in neuroparenchymal white matter tracts. Normal appearing white matter adjacent to MS lesions has been shown to have abnormally reduced fractional anisotropy on several studies (35). Conventional MRI often underestimates the cortical gray matter involvement. Assessment of cortical lesions maybe enhanced with 3D FLAIR imaging, double inversion recovery pulse sequence (DIR), phase sensitive inversion recovery (PSIR) sequences and 7T MRI.

Limitations of Conventional MRI

Conventional MRI is a qualitative MR technique. The pathological lesion is traditionally described in the form of deviation in inherent tissue properties like longitudinal and transverse relaxation rates (R1 and R2 respectively), diffusion weighting, proton density (PD) etc in relation to the normal surrounding tissue. So, a pathological lesion is typically described as T2 hyperintense or T1 hypointense compared to the normal gray matter. These relative terms of hyperintensity or hypointensity are not absolute and imply a subjective interpretation of the lesion behaviour. In addition, several different pulse sequences (depending on the contrast studies like T1, T2, PD etc) are required to delineate contrast deviation vis-à-vis normal surrounding tissue in clinical routine (8). Further, the image characteristics used to describe these lesions vary based on several acquisition parameters and variations in individual MR scanner machine (36).

On the other hand, discrete quantification of inherent tissue parameters like proton density (PD), R1 and R2 relaxation rates etc allow more objective and quantifiable pathological evaluation, independent of acquisition parameters and MR scanner variables (36). As an additional benefit, quantitative MRI may enable automated segmentation of images and the pathology can be expressed in absolute numbers – devoid of relative terms like hypointense or hyperintense (8).

Quantitative MR methods

Several MR techniques have been described enabling rapid quantification of T1 relaxation rate (R1), T2* relaxation rate ($R2^*$), T2 relaxation rate (R2) and proton density (PD) in last two decades, however, most of these have been described in research arena with limited utilization in clinical setting (37–42) largely due to inhibitory long scanning duration or low signal to noise ratio (SNR). In the last few years, there has been a substantial progress in development of novel quantitative MR techniques wherein, some of them can be utilized to obtain absolute quantitative values of R1, R2, PD and B1 inhomogeneity of entire imaging volume with acceptable resolution and within clinically practical scan times (8).

Another persistent issue with routine clinical adoption of quantitative MR methods that should not be underestimated is the lack of experience in using these absolute values of T1, T2, PD etc to study and describe disease processes in the clinical radiology workflow. The physicians are used to evaluating conventional contrast-weighted images for disease evaluation and may not be comfortable initially bypassing this route and relying solely on quantitative values (8).

Both these issues have been attempted to be addressed in the following paragraphs by introducing different quantitative MR techniques, each having its own strengths and limitations. A few imaging techniques allowing for simultaneous and accurate quantitative assessment of R1, R2 and PD have been described (43,44), as exemplified below:

IR-TrueFISP

This technique was initially described as rapid T1 quantification method (45). In this method, segmental TrueFISP data are acquired in an inversion recovery (IR) sequence at different time points. Thus, several images with different signal recovery weightings are generated and

subsequently fitted to an inversion recovery (IR) curve to estimate T1 values. For simultaneous acquisition of T1, T2 and PD parameters, two solutions were proposed by the authors. First, the acquired data could be fitted on a simplified analytical model that led to introduction of MDME sequence described below. Alternatively, dictionary matching of numerical Bloch simulations may be used to define quantitative parameters from the acquired data as described in MRF technique below.

MRF

MR fingerprinting is another technique that allows simultaneous measurement and quantification of T1, T2 and M0 parameters by dynamically and continuously varying flip angle (FA) and repetition time (TR) in pseudorandom manner to create a unique "fingerprint" of the imaged voxel (46,47). This unique fingerprint for each voxel is matched with a dictionary of pre-labelled tissue parameters information to generate property set of that particular voxel. A highly undersampled acquisition is utilized for MRF to reduce scan times. Dictionaries can be generated by using numerical Bloch equations. High repeatability and reproducibility of T1 and T2 quantitative values generated from MRF protocol was noted in ISMRM MRI phantom (48) and in healthy controls across varied MR scanners (49,50).

MDME (Synthetic MRI/SyMRI)

SyMRI pulse sequence

As per synthetic MRI white paper (51), synthetic MRI enables fast and accurate quantification of R1, R2, PD as well as B1 field by implementing a 2D, multi-dynamic, multi-echo (MDME), fast spin echo (FSE) pulse sequence performed using an interleaved slice-selective 120 degree saturation (51). The saturation and acquisition act at representative slices m and n respectively, where m and n represent separate slices in the planned stack. Thus, by controlling the choices

of m and n, it is possible to vary the effective delay times between saturation phase and acquisition phase.

Four different choices of m and n are implemented by the pulse sequence automatically, without any user inputs, resulting in four different delay times (TI). The number of acquisition echoes is fixed at two, at two separate echo times (TE). This results in each MDME sequence generating eight images per slice acquisition (four saturation delays at two separate echo times) shown in Figure 1 below (51).

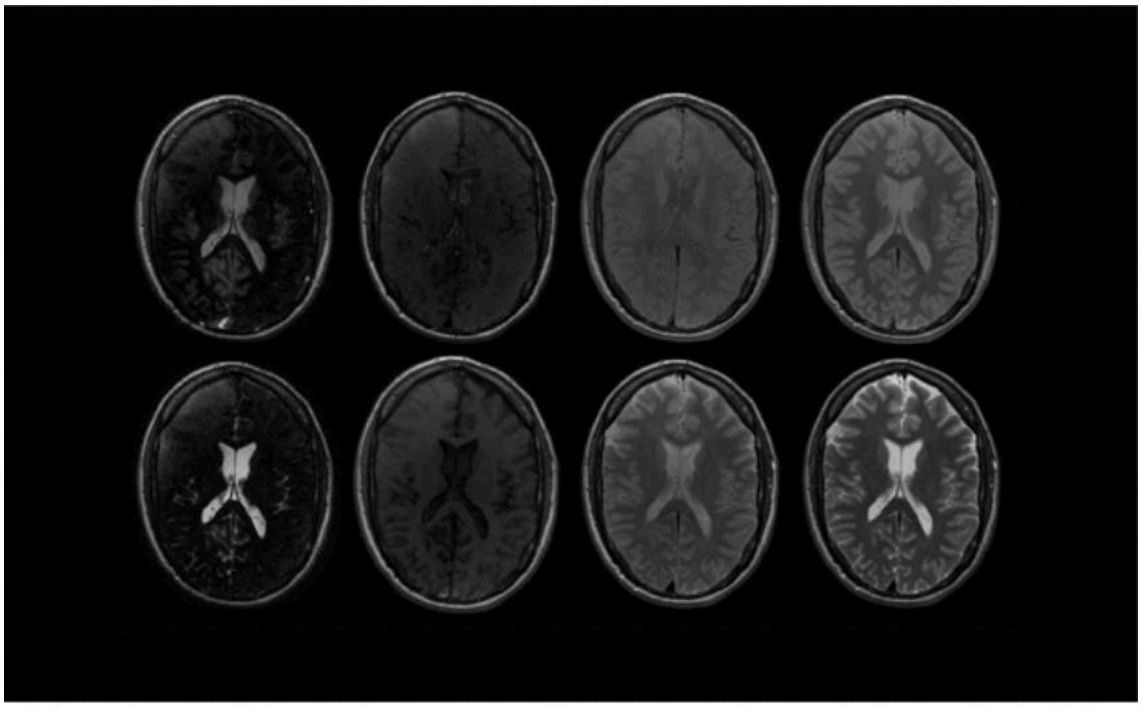

Figure 1: Raw MDME images generated from a single slice.

SyMRI post-processing

As per synthetic MRI white paper (51), synthetic MRI algorithm performs complex mathematical modelling and calculates the T1 and T2 relaxation values at each pixel of 8 images per slice. Further, proton density (PD) values are calculated from following equation (51) (Figure 2):

$$S = A \cdot PD \cdot \exp(-TE/T_2) \cdot \frac{1-[1-\cos(B_1\theta)]\cdot\exp(-TI/T_1)-\cos(B_1\theta)\cdot\exp(-TR/T_1)}{1-\cos(B_1\alpha)\cdot\cos(B_1\theta)\cdot\exp(-TR/T_1)}$$

where A represents intensity scaling factor, θ represents 90 degrees flip angle and ∝ indicates 120 degrees saturation pulse angle (51). Post-processing time is less than 10 seconds.

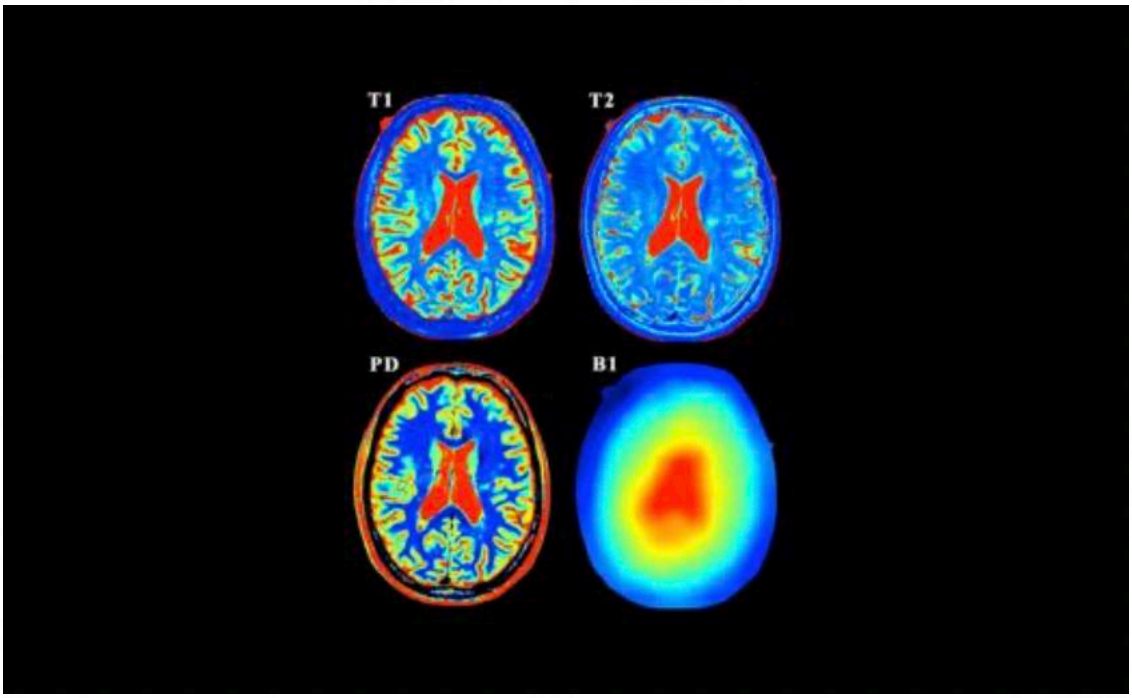

Figure 2: Processed MDME images representing SyMRI generated T1 and T2 relaxation times, PD and B1 field maps (51)

Generation of synthetic images

After calculating T1, T2 and PD values, normal MRI images can be generated by calculating the expected signal intensity S as a function of TE, TR and an inversion pulse with inversion delay time TI.

For T1 and T2 FSE images, θ is 0 and equation becomes (Figure 3):

$$S = PD \cdot \exp(-TE/T_2) \cdot (1 - \exp(-TR/T_1))$$

For IR-FSE images like FLAIR, θ is 180 degrees and equation becomes (Figure 3):

$$S = PD \cdot \exp(-TE/T_2) \cdot (1 - 2 \cdot \exp(-TI/T_1) + \exp(-TR/T_1))$$

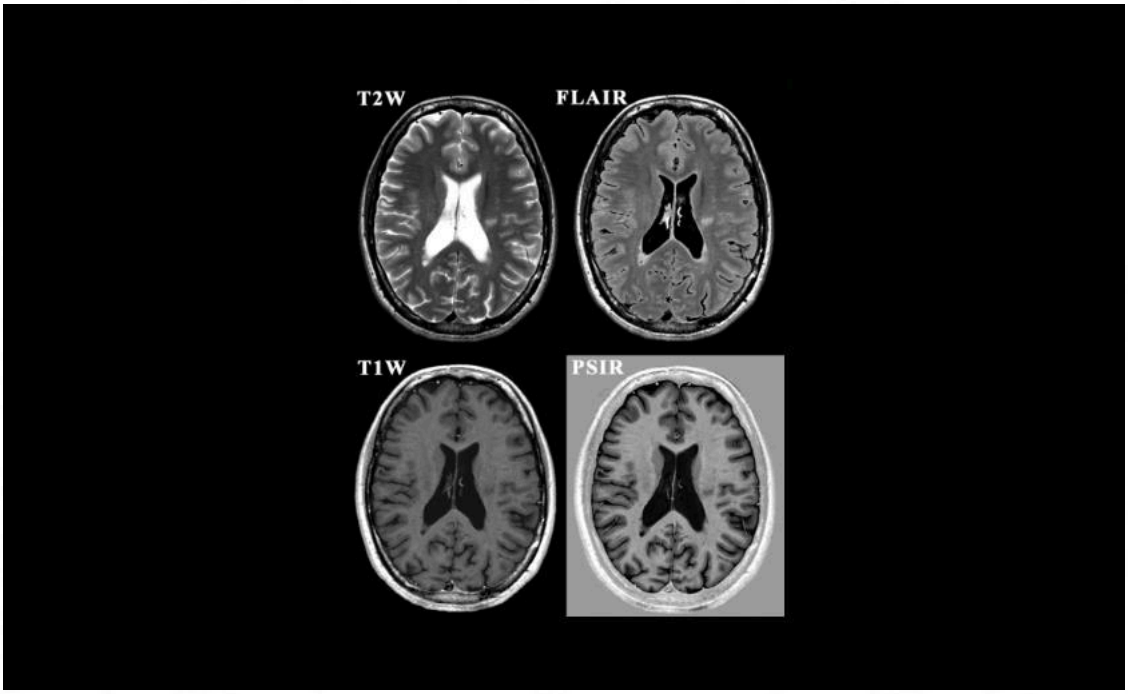

Figure 3: Synthetic T2, T1 FSE and FLAIR, PSIR images (51)

Tissue segmentation

Synthetic tissue segmentation maps can be derived from T1, T2 and PD synthetic maps and resulting white and gray matter, cerebrospinal fluid (CSF) along with myelin segmentation are performed by the software without any user interaction. The segmentation is carried out by post-processing software based on a partial volume model in which each voxel is assumed to contain 0 to 100% of a specific tissue type. This method makes segmentation process

independent of flip angles and imaging resolution. The above segmentation technique has been validated by a few earlier studies (10,52). An example of tissue segmentation maps synthesized is given in figure 4 below.

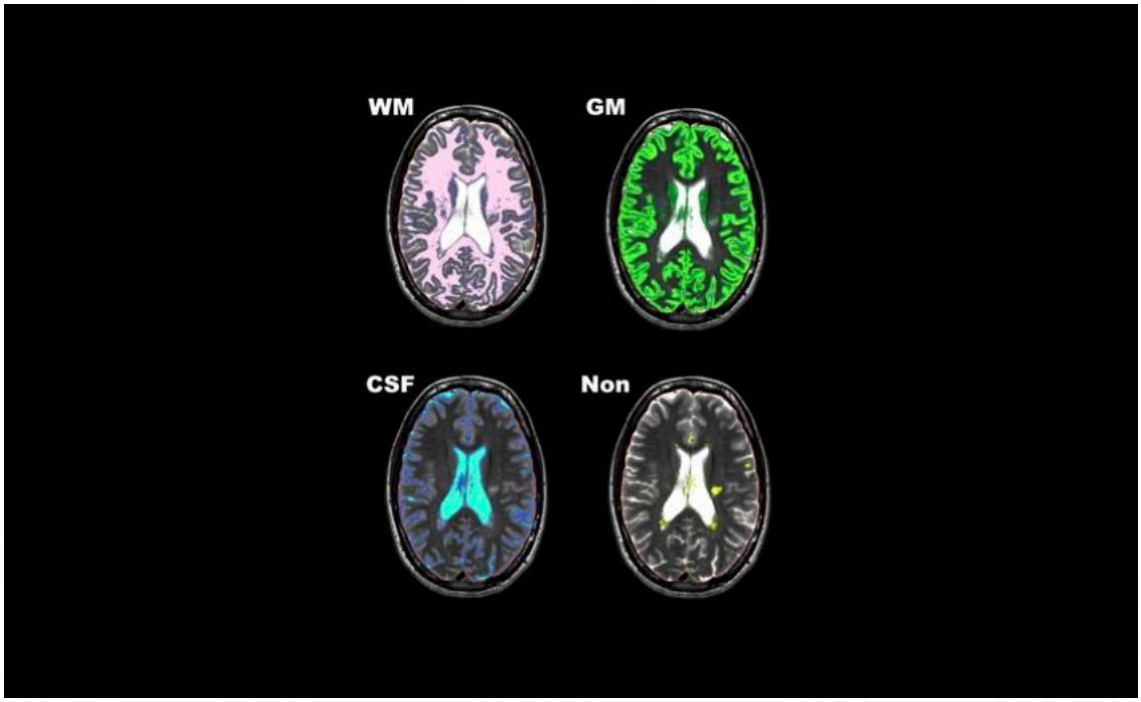

Figure 4: Tissue segmentation maps derived from synthetic MRI (51)

Brain tissue characterisation & measurement

SyMRI post processing tool incorporates automated characterisation & measurement of brain tissue components like cerebrospinal fluid (CSF), gray matter (GM), white matter (WM) as well as non-gray/white matter/cerebrospinal fluid (NoN) within a few seconds without any user intervention. This volumetric information is available for entire intracranial volume, per region of interest (ROI) and per slice. This quantitative data is then utilised to calculate useful ratios like brain parenchymal fraction (BPF) from intracranial volume (ICV), brain tissue and cerebrospinal fluid (CSF) volumes. BPF has been demonstrated as a useful quantitative parameter for assessing neuroparenchymal volume loss/atrophy in several neurodegenerative conditions like multiple sclerosis (MS) and dementias.

Myelin assessment & quantification

Myelin plays an indispensable role in maintaining integrity of axonal fibres and enables smooth and accelerated propagation of action potentials across nerve fibres (53–55). Multiple MR techniques have been devised in recent past to evaluate and study pathology of demyelinating conditions like multiple sclerosis (MS) (55). Myelin imaging holds promise in prognosticating and monitoring therapeutic responses in clinical scenarios, especially in demyelinating conditions like MS. However, imaging based myelin estimation still faces hurdles as there is no established benchmark for myelin assessment and quantification. Myelin water fraction (MWF) is a widely researched as well as validated quantitative measure that allows indirect myelin assessment in brain parenchyma (56).

Myelin estimation using quantitative SyMRI based quantitative parameters was proposed initially in 2016 (11). Herein, the myelin model assumes four intracranial segregated compartments – myelin volume fraction (MVF), cellular volume fraction, free water fraction and excess parenchymal water volume fraction (11). This model further assumes that each of the above compartments has a specific set of distinct parametric values like PD, R1 and R2 that result in effective PD, R1 and R2 of a specific voxel while exchanging magnetisation with adjacent compartments. Myelin volume fraction (MVF) derived from synthetic MRI correlates well with histology specimens obtained from normal brains (57), pathological brains with multiple sclerosis and with good reproducibility between scanner models (58). Clinical applications of MVF have been studies in Sturge-Weber syndrome (59), multiple sclerosis (2,60) and CADASIL (57).

Clinical Applications of Synthetic MRI

Brain metastases

The most common neoplastic aetiology involving the brain parenchyma is metastatic deposits secondary to non-neurologic malignancies. Gadolinium contrast MRI is indispensable for identifying intracranial metastatic deposits - postcontrast T1-w images and T1 Inversion Recovery (IR) images are routinely used for the same. Hagiwara et al compared synthetic MRI against conventional MRI in evaluating intracranial metastatic deposits (61). The CNR (contrast to noise ratio) was significantly higher for synthetic T1 IR images compared to synthetic T1 weighted and conventional T1 IR images. Also, many more lesions were picked up on synthetic T1 IR imaging as compared to synthetic T1 weighted and conventional T1 IR images although statistically significant difference could not be established (61).

Further, as has been shown by several recent studies, contrast enhanced conventional FLAIR images are best suited for picking up meningeal metastatic deposits (62). The added benefit of synthetic MRI lies in the fact that contrast enhanced synthetic FLAIR images can be generated automatically even if meningeal carcinomatosis was not suspected before the acquisition, thereby enabling higher rates of detection.

Sturge-Weber Syndrome

Sturge-Weber Syndrome is one of the rarer neurocutaneous syndromes affecting the superficial cortical and meningeal micro-vasculature. The syndrome is characterized radiologically and pathologically by the presence of leptomeningeal angiomatosis - most frequently involving the posterior parieto-occipital region. Ipsilateral facial port wine stain (cutaneous vascular malformation) frequently distributed along the V1 (ophthalmic) division of trigeminal nerve is commonly associated with this condition (63). Contrast enhanced MRI often reveals prominent

leptomeningeal postcontrast enhancement in the involved loebs. Hagiwara et al in there paper were able to demonstrate ipsilateral dural enhancement in addition to the leptomeningeal enhancement in a patient of Sturge-Weber Syndrome (SWS) using postcontrast synthetic double inversion recovery (DIR) sequence that nulls the signal of cerebrospinal fluid and adjacent calvarium marrow fat (64). In this particular case, dural enhancement likely represents dural angiomatosis that has been shown in a few pathological specimens of Sturge-Weber syndrome (SWS) but rarely reported upon in the neuroradiology literature.

Normal Pressure Hydrocephalus (NPH)

Idiopathic normal pressure hydrocephalus (iNPH) is characteristically described as clinical triad of cognitive dysfunction, apraxic gait and urinary incontinence. Numerous conventional MR imaging findings suggestive of this disease have been described such as diffuse ventricular enlargement (measured by the Evan's index) in absence or out of proportion to cortical atrophy, disproportionately enlarged subarachnoid space hydrocephalus (DESH pattern) characterized by tight convexity and medial subarachnoid paces along with disproportionately enlarged Sylvian fissures, periventricular white matter changes and increased aqueductal stroke volume as determined by phase-contrast MR studies. The quantitative parameters like the Evan's index has a poor sensitivity in predicting response to shunting in iNPH patients. After shunting, a significant number of patients may show clinical improvement without any significant change in the Evan's index. Virhammar et al (65) evaluated iNPH patients using synthetic MRI before as well as after ventricular shunting. Post lumbar puncture, significant reduction in lateral ventricular volumes was noted as measured by manual segmentation. Similarly, reduced CSF volume and increased brain parenchymal fraction (BPF) as measured by synthetic MRI was also noted. The study showed that cerebrospinal fluid (CSF) volume and brain parenchymal fraction (BPF) values correlated significantly with the lateral ventricular volume as measured

by manual segmentation. The authors also proposed that these quantitative parameters measured by synthetic MRI maybe utilized in objective monitoring of the disease course as well as therapeutic response in cases of normal pressure hydrocephalus (65).

Multiple Sclerosis

As discussed above, synthetic MRI is one of the most robust quantitative MRI techniques that enables accurate evaluation and quantification of R1 and R2 relaxation rates along with proton density measurements in clinical setting. Also, automated, user independent brain tissue segmentation into white matter (WM), gray matter (GM) and cerebrospinal fluid (CSF) can be performed using these quantitative values. Further, synthetic MRI image contrasts like T1, T2 and FLAIR weightings can be derived by applying mathematical expressions to the given quantitative parameters.

Few studies comparing the image quality of conventionally acquired T1, T2 and FLAIR images against similar contrast weightings derived from synthetic MRI have demonstrated that synthetic T1 and T2 weighted images are comparable to conventional images but synthetic FLAIR images are of slight inferior quality (9).

Tanenbaum et al (66) in one of the largest prospective, randomized study comparing synthetic and conventional imaging in different neurological diseases demonstrated statistical non-inferiority regarding overall diagnostic quality of synthetic MRI compared to conventional MRI for T1, T2, PD, STIR, T1 FLAIR and T2 FLAIR weighted images. Conventional and synthetic MR sequences demonstrated comparable quality and artifacts for T1, T2, PD and STIR weighted images while synthetic FLAIR images had more number of artifacts compared to conventional FLAIR images.

Granberg et al (9) in their clinical feasibility study on SyMRI in multiple sclerosis (MS) posited that synthetic MRI maybe feasible as complementary or even an alternative to conventional PD, T1 and T2 weighted images in multiple sclerosis. This study showed good agreement between volumes of MS plaques and total lesion count. They also commented that pulsation artifacts diminish the image quality of synthetic FLAIR images and need proper redressal before substituting conventional FLAIR images. They conclusively established that synthetic MRI derived volumetric measurements are in agreement with other commonly used volumetric softwares (FreeSurfer, SPM and FSL) and had the least repeat measurement errors for brain volume (BV), brain parenchymal fraction (BPF) and intracranial volume (ICV) among all the examined methods (9).

Krauss et al (67) in their conventional versus synthetic MRI in MS comparative study demonstrated no statistically significant difference in intra- and inter-observer agreement in the detection of plaques between the two techniques. The total lesion count in both conventional as well as synthetic MRI images was also comparable. The SNR was better in synthetic T2 and FLAIR images in comparison to conventional MR images that was attributed to the selection of bigger voxel size in synthetic MRI images (67).

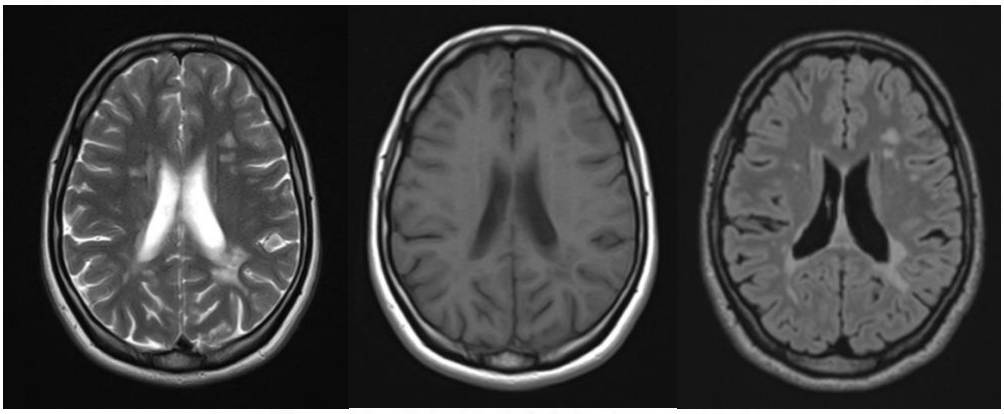

Figure 5: Example of synthetic MRI T2, T1 (non-contrast) and FLAIR images in a multiple sclerosis patient.

3 MATERIALS AND METHODS

This study is a prospective, cross-sectional, observational study. Consecutive suspected or confirmed multiple sclerosis (MS) cases presenting at Neurology clinic underwent conventional MRI with contrast along with synthetic MRI sequence of brain at 1.5T Siemens MRI scanner (Siemens Healthcare Ltd).

Subjects

43 consecutive patients with clinically suspected or confirmed multiple sclerosis presenting to Neurology Clinic at SCTIMST, Trivandrum, Kerala from Jun 2020 till Jun 2022 were included in this prospective, observational, cross-section study. The selected patients underwent conventional MRI with gadolinium contrast along with synthetic MRI sequence of brain at 1.5T MRI scanner (Siemens Healthcare Ltd). Prior Institutional Ethics Committee approval was obtained, Informed consent was taken from all subjects.

Inclusion and Exclusion criteria

(i) Inclusion Criteria:

1. Fulfilment of 2017 revisions of McDonald criteria for relapsing remitting or progressive multiple sclerosis.
2. Age 18 years or above.
3. Consenting to participate in the study.

(ii) Exclusion Criteria:

1. Claustrophobic patient.
2. Allergy to gadolinium-based contrast agent.
3. Lesion size < 3mm or > 30 mm on conventional T2W/FLAIR MR images.
4. Cervico-medullary junction, optic nerve and spinal cord lesions due to small lesion size and likely region of interest (ROI) placement errors.
5. Inadequate ancillary investigations to satisfactorily rule out alternate clinical diagnoses.

MR Image Acquisition

Imaging was acquired on 1.5 Tesla MR imaging scanner (Magnetom Avanto Fit, Siemens Healthcare GmBH, Erlangen, Germany) on a 20 channel phased array head coil. Each subject underwent conventional MRI (multiple sclerosis institutional protocol) including 3D FLAIR, axial spin echo T1 and T2, SWI, DWI, sagittal T2 followed by post contrast coronal T1 spin echo sequences (approximate delay of 10 minutes after administering contrast agent). T2 spine echo imaging for optic nerves and spinal cord was also performed as part of the institutional multiple sclerosis protocol. Synthetic MRI pulse sequence was performed in every patient before administering contrast.

Conventional MRI brain had following acquisition parameters:

- T2 FLAIR: 3D acquisition; FOV 202 x 256 mm; voxel size 1 mm^3; TE 335 ms; TR 5000 ms; TI 1600 ms; total scan duration 5 min 37 seconds
- T2 FSE: Axial 2D acquisition; 25 sections; FOV 244 x 384 mm; voxel size 0.6 x 0.6 mm; TR 4500 ms; TE 111 ms; total scan duration 42 seconds
- T1 SE (pre-contrast): Axial 2D acquisition; 25 sections; FOV 146 x 256 mm; voxel size 0.9 x 0.9 mm; TR 383 ms; TE 8.9 ms; total scan duration 1 min 11 seconds

All conventional MRI images had section thickness 4 mm and an inter-slice gap of 2.4 mm.

- T1 FSE (post contrast): Coronal 2D acquisition; 35 sections; FOV 174 x256 mm; voxel size 0.9 x 0.9 mm; TR 590 ms; TE 9.5 ms; scan duration 3 min 31 seconds

All post contrast coronal MRI images had section thickness 3 mm and an inter-slice gap of 0.8 mm.

Synthetic MRI is a 2D, multi-section, multi-echo and multi-delay quantitative MRI pulse sequence with following parameters:

- Axial 2D; FOV 176 x 320 mm; 30 sections; voxel size 0.7 x0.7 mm; TE (21 and 96 ms); TR 4200 ms; TI 25 ms; flip angle 150 degrees; scan time 5 min 53 seconds.

All synthetic MRI images had section thickness 4 mm and an inter-slice gap of 1 mm.

Post-processing and ROI placement

Post-processing of synthetic MRI pulse sequence dataset was performed on a laptop computer by utilising SyMRI software v11.2 (SyntheticMR, Linkoping, Sweden) and total post-processing time was less than a minute per case. The software generated quantitative parametric maps of R1, R2, PD and myelin correlated volume (MyC) (Fig 8). These parametric maps were used to generate synthetic contrast images namely – T1, T2, T1 FLAIR, T2 FLAIR, PD, DIR (double inversion recovery), PSIR (phase sensitive inversion recovery).

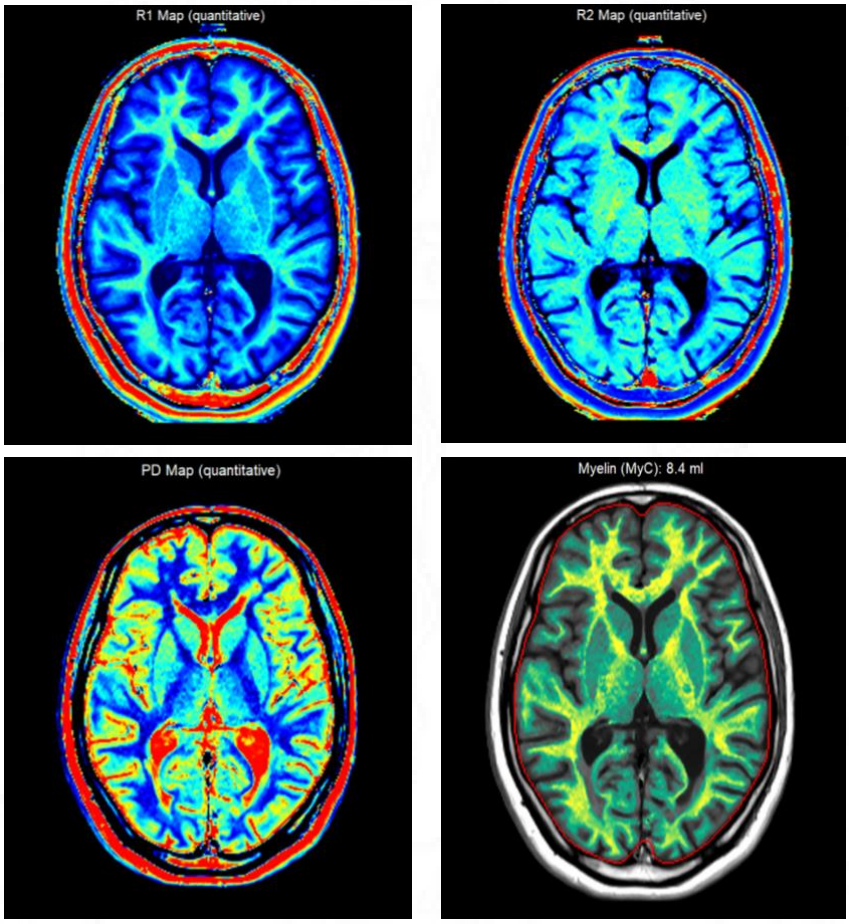

Figure 6: SyMRI generated R1, R2, PD and Myelin maps in a representative patient.

For each case, conventional FLAIR, T2, T1, post contrast T1 sequences and synthetic FLAIR sequences were studied by displaying them side by side. Multiple sclerosis plaques were identified by visual inspection using conventional neuroradiology criteria and classified as per their location – periventricular white matter (contacting ependymal lining), deep white matter,

infratentorial and cortical-juxtacortical. The MS plaques were further divided into enhancing or non-enhancing lesions.

Regions of interest (ROI) were carefully placed on synthetic FLAIR images within MS plaques of >3 mm and < 30 mm largest dimension (as per the inclusion criteria) corresponding to non-enhancing and enhancing MS plaques on conventional MR imaging respectively, slightly inside the outer rim to limit partial volume effects from adjacent structures.

Regions of interest (ROI) placement was also done in synthetic FLAIR images in normal-appearing white matter (NAWM) of contralateral neuroparenchyma corresponding as far as possible to the plaque location, if feasible.

Quantitative parameters namely R1, R2, PD and myelin correlated volume (MyC) from each ROI was entered in master excel sheet alongside relevant clinical data pertaining to each patient.

STATISTICAL ANALYSIS

The data thus collected was compiled using Microsoft excel. The data was analysed using Statistical Package for Social Services (SPSS v20). The qualitative variables were described using frequencies and percentages. The continuous variables were described using mean and standard deviations. Sensitivity and specificity at different cut off levels was performed using receiver operating characteristic (ROC) curves analysis. Finally, logistic regression analysis was performed for differentiating between enhancing and non-enhancing plaques.

4 RESULTS

A total of 48 MR examinations were carried out for the purpose of current study, eight of these had both non-enhancing as well as contrast enhancing MS plaques. Forty examinations had no contrast enhancing lesions. Out of total 43 patients included in the study, one patient underwent three MR examinations and three patients underwent two MR examinations respectively, during the course of study.

Table 3. Distribution of study group according to age group

Age group	Frequency	Percent
Less than 20 y	5	10.4
21 – 30 y	15	31.3
31 – 40 y	19	39.6
41 – 50 y	8	16.7
51 – 60 y	1	2.1
Total	48	100

Chart 1. Distribution of study group according to age group

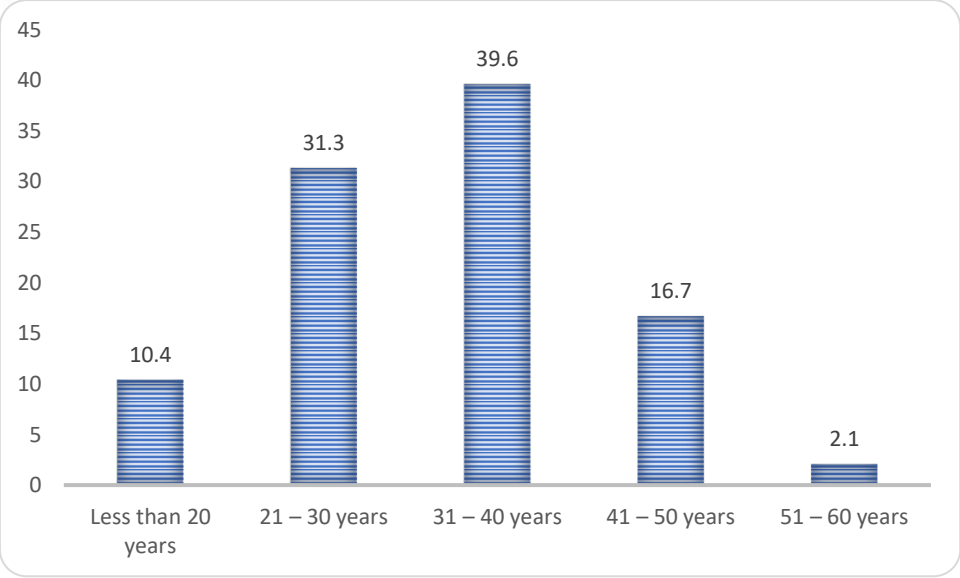

About 39.6% of the cases in this study were aged between 31 – 40 years. This was followed by 21 – 30 years and 41 - 50 years.

Table 4. Distribution of study group according to sex

Sex	Frequency	Percent
Male	16	33.3
Female	32	66.7
Total	48	100

Chart 2. Distribution of study group according to sex

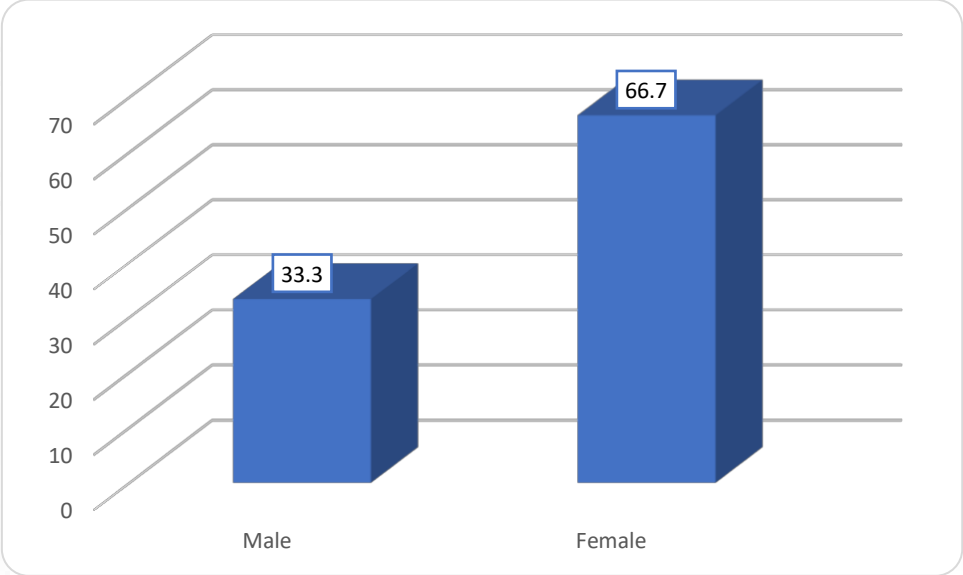

About 66.7% of the cases in this study were females and 33.3% were males.

Table 5. Distribution of study group according to duration of disease

Duration of the disease	Frequency	Percent
Less than 2 years	9	18.8
2 – 5 years	16	33.3
More than 5 years	23	47.9
Total	48	100

Chart 3. Distribution of study group according to duration of disease

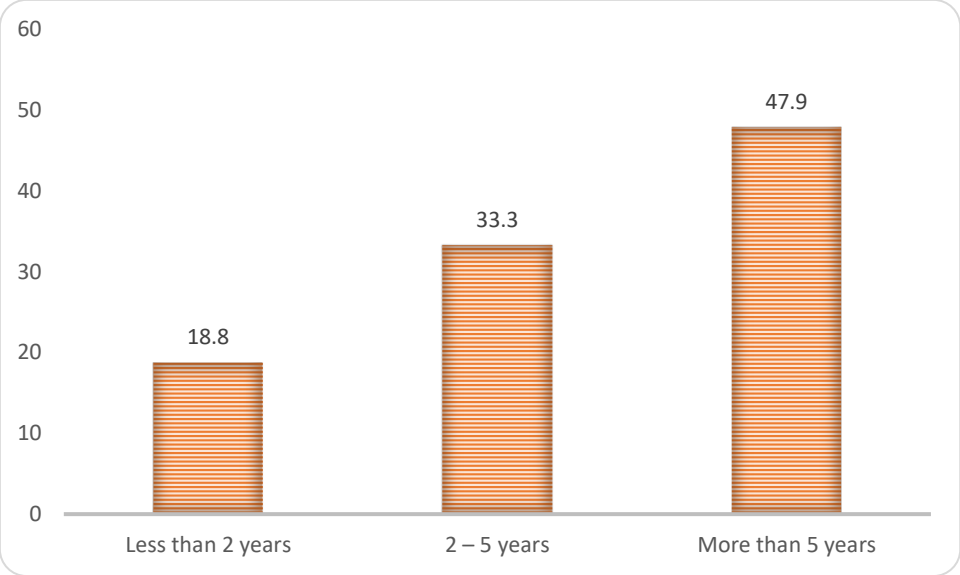

The duration of the disease was more than 5 years in 47.9% of the cases followed by 2 – 5 years in 33.3% of the cases and less than 2 years in 18.8% of the cases.

Table 6. Distribution of study group according to type of MS lesions

Type of study	Frequency	Percent
Non-enhancing	430	62.0
Contrast enhancing	43	6.3
NAWM	219	31.7
Total	692	100

Chart 4. Distribution of study group according to type of study

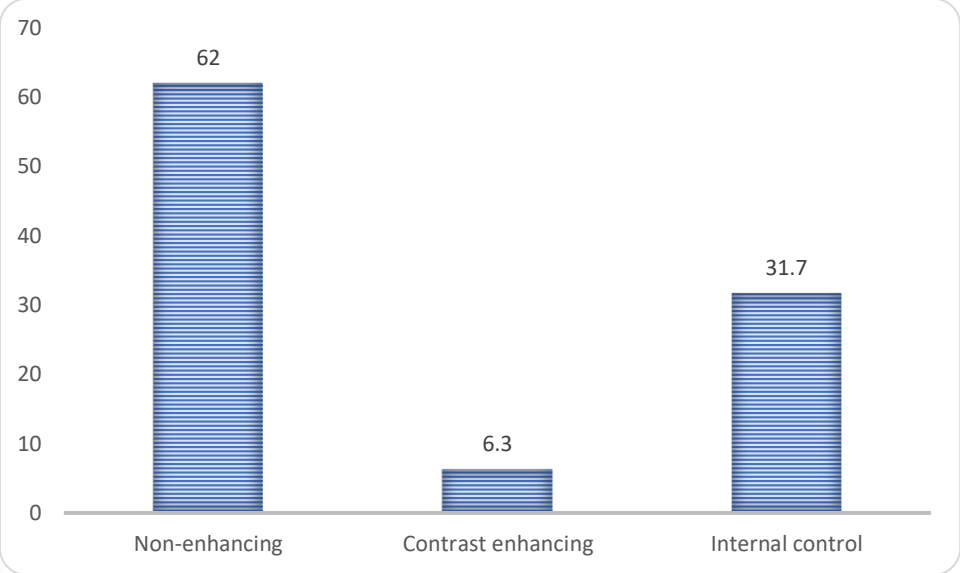

This study had shown that, about 62.0% of the studies were non – enhancing plaques, 6.3% were contrast enhancing plaques and 31.7% were internal controls.

Table 7. Distribution of study group according to MS lesion location

Location	Contrast enhancing plaques n (%)	Non-contrast enhancing plaques n (%)
C – JC	14 (32.6)	125 (29.1)
Deep	1 (2.3)	50 (11.6)
IT	4 (9.3)	78 (18.1)
PVWM	24 (55.8)	177 (41.2)
Total	43 (100)	430 (100)

χ^2 value=6.082 df=3 p value=0.108, NS

Chart 5. Distribution of study group according to type of study and location

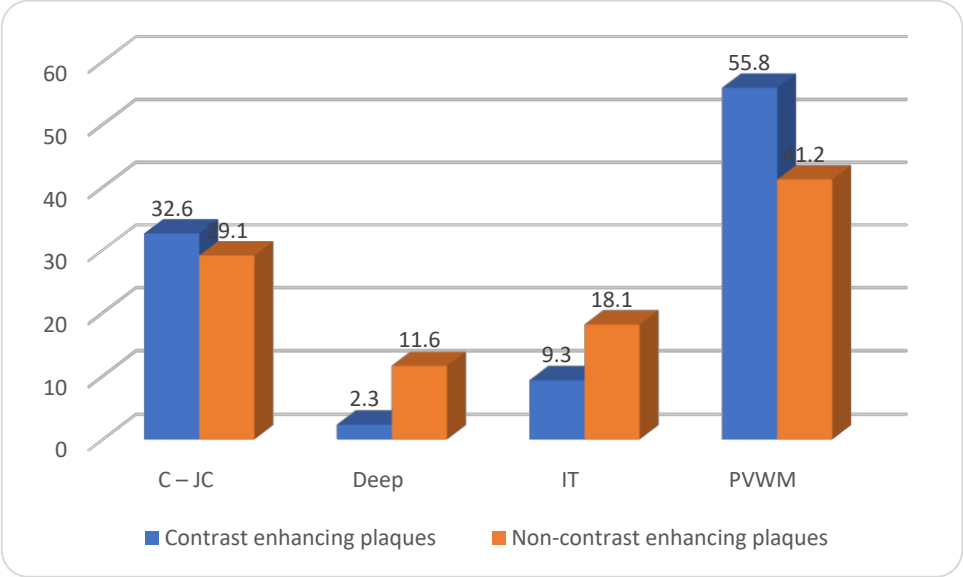

About 55.8% of the cases with contrast enhancing plaques and 41.2% with non-contrast enhancing plaques had lesions in PVWM in this study. This difference was not statistically significant,

Table 8. SyMRI derived quantitative parameters of normal – appearing white matter, enhancing and non-enhancing MS plaques

Type of lesion	R1 Mean ± SD	R2 Mean ± SD	PD Mean ± SD	MyC Mean ± SD
Contrast enhancing (C)	1.06 ± 0.22	9.29 ± 1.62	81.42 ± 9.14	2.79 ± 3.46
Non-enhancing (N)	0.91 ± 0.16	8.28 ± 1.49	85.01 ± 6.35	5.12 ± 5.37
NAWM	1.38 ± 0.19	12.04 ± 0.98	69.27 ± 5.26	24.2 ± 7.81
Difference C/N	0.15	0.24	1.05	0.86
P value	0.000, Sig	0.000, Sig	0.000, Sig	0.000, Sig

Enhancing lesions had significantly higher mean R1, R2 values and significantly lower mean PD values compared to non-enhancing lesions. Further, normal-appearing white matter (NAWM) had significantly higher mean R1, R2 and significantly lower PD than

enhancing lesions. For enhancing lesions, mean R1 value was 1.06 s^{-1}, mean R2 value was 9.29 s^{-1} and mean PD value was 81.42%. For non-enhancing lesions, mean R1 value was 0.91 s^{-1}, mean R2 value was 8.28 s^{-1} and mean PD value was 69.27%. Normal-appearing white matter had mean R1 value of 1.38 s^{-1}, mean R2 value of 12.01 s^{-1} and mean PD value of 69.27%.

Charts 6-8 show distribution of mean R1, mean R2 and mean PD for enhancing vs non-enhancing lesions. As is evident, contrast enhancement was extremely rare in lesions with mean R1 below 0.75 s^{-1} (sensitivity 97.4%). Similarly, enhancing lesions were uncommon below mean R2 value of 7.18 s^{-1} (sensitivity 91.9%).

Tables 10-12 show sensitivity and specificity profile for various cut-offs in mean R1, R2 and PD values for discriminating enhancing from non-contrast enhancing MS plaques. When sensitivity and specificity for all possible thresholds was combined in a receiver operating characteristic (ROC) analysis, the area under ROC curve (AUC) respectively for mean R1 and R2 values was 0.667 and 0.656 that was statistically significant in differentiating contrast enhancing and non-contrast enhancing lesions. But PD had an AUC value of 0.411 that was not statistically significant.

Chart 6. Histogram showing mean R1 values of contrast enhancing and non-contrast enhancing lesions

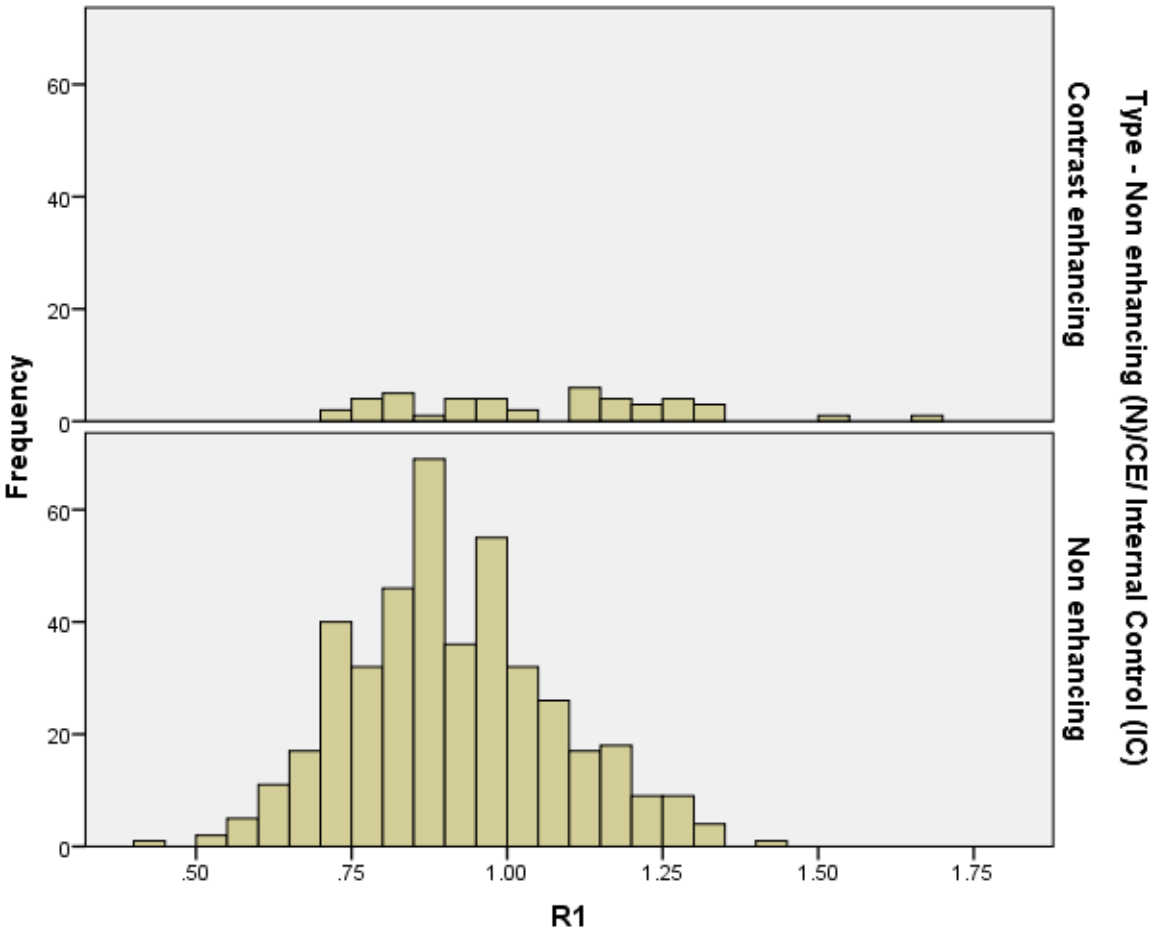

The histogram shows that R1 values of enhancing lesions were higher than the non-enhancing lesions.

Chart 7. Histogram showing mean R2 values of contrast enhancing and non-contrast enhancing lesions

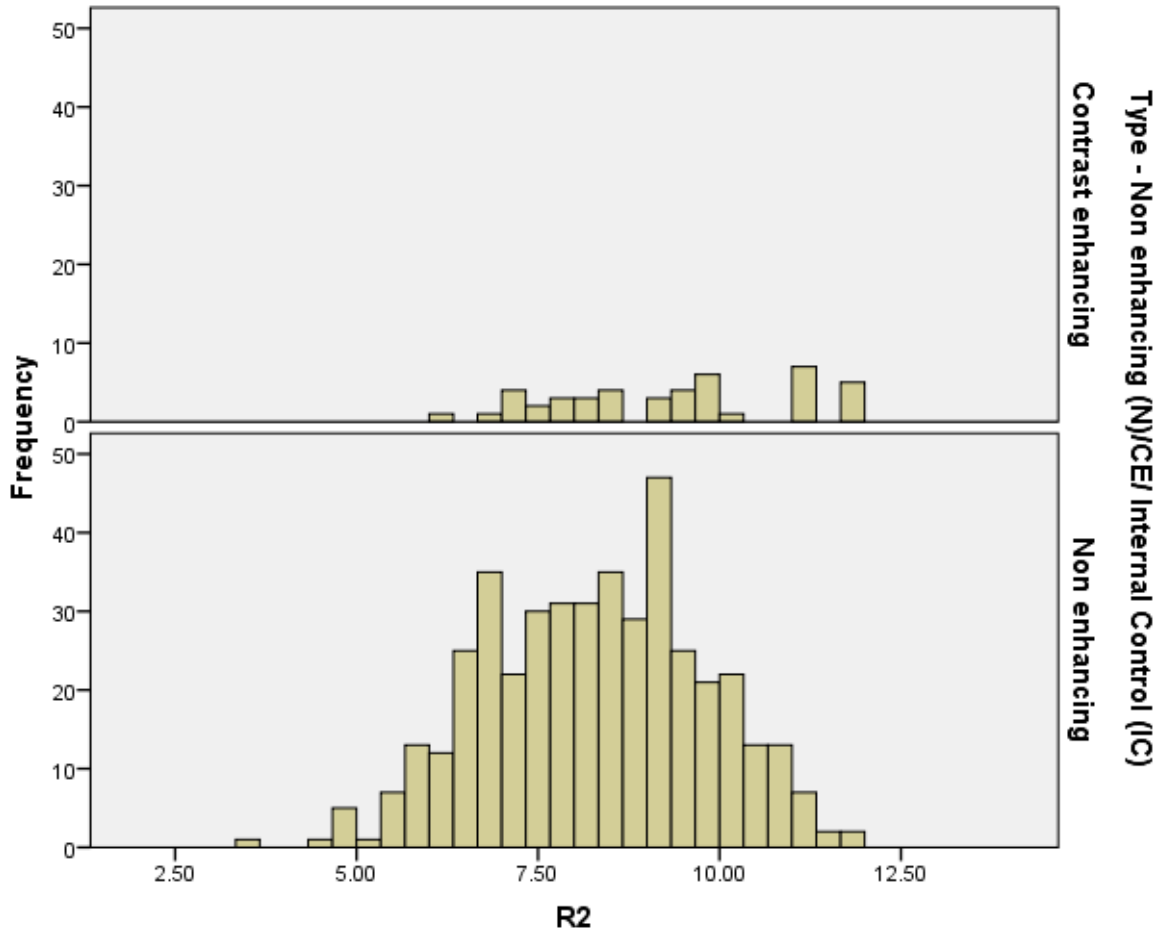

The histogram shows that R2 values of enhancing lesions were higher than the non-enhancing lesions.

Chart 8. Histogram showing mean PD values of contrast enhancing and non-contrast enhancing lesions

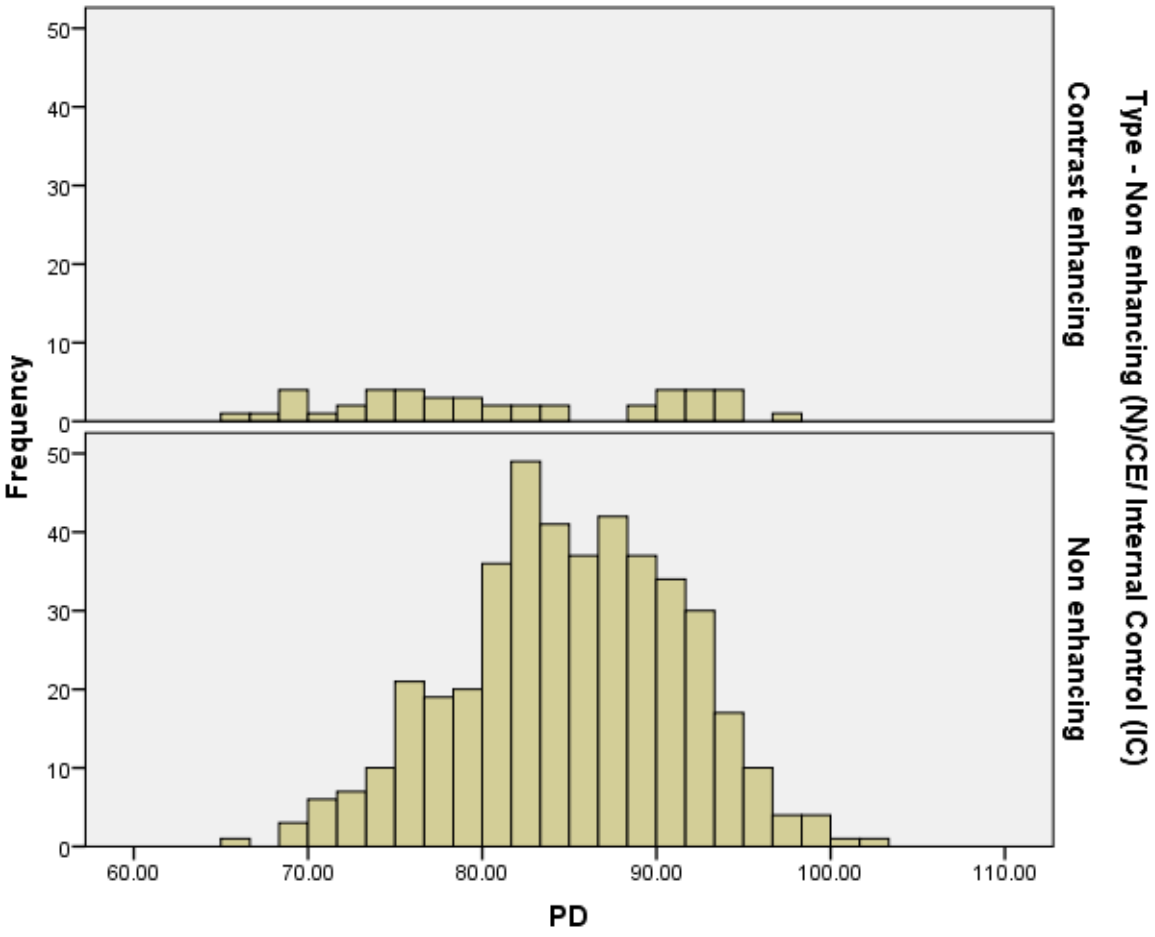

The histogram shows that PD values of non-enhancing lesions were higher than the contrast enhancing lesions.

Table 9. Area under curve values of contrast and non-contrast enhancing lesions

Area Under the Curve

Test Result Variable(s)	Area	Std. Error[a]	Asymptotic Sig.[b]	Asymptotic 95% Confidence Interval	
				Lower Bound	Upper Bound
R1	.667	.049	.000	.570	.764
R2	.656	.047	.001	.563	.748
PD	.411	.059	.059	.295	.528
MyC	.371	.043	.006	.288	.454

The test result variable(s): R1, R2, PD, MyC has at least one tie between the positive actual state group and the negative actual state group. Statistics may be biased.

a. Under the nonparametric assumption

b. Null hypothesis: true area = 0.5

The area under curve of R1, R2 and MyC values were 0.667, 0.656 and 0.371 which had significant difference between contrast enhancing and non-enhancing lesions.

Table 10. Cut off values of R1

R1 (test results – cut off values)	Sensitivity (%)	Specificity (%)
0.48	100	0.2
0.73	100	13.7
0.75	97.7	17.2
0.8	90.9	25.1
0.81	86.4	26.5
0.83	84.1	31.4
0.84	77.3	35.6
0.86	75.0	41.2
0.91	72.7	56.7
0.93	68.2	57.4
0.95	65.9	60.0

The sensitivity and specificity of R1 values at a cut off of 0.48 was 100% and 0.2% and a cut off value of 0.95, sensitivity was 65.9% and specificity was 60.0%.

Table 11. Cut off values of R2 values

R2 (test results – cut off values)	Sensitivity (%)	Specificity (%)
2.41	100	0
6.19	100	7.8

6.91	97.7	20.2
7.08	95.5	24.7
7.15	93.2	25.8
7.18	90.9	26.3
7.31	88.6	28.4
7.42	86.4	29.8
7.6	84.1	34.4
7.79	77.3	39.5
8.17	75.0	46.0
8.18	72.7	46.7
8.22	70.5	47.9
8.46	65.9	52.6

The sensitivity and specificity of R2 values at a cut off of 2.41 was 100% and 0% and a cut off value of 8.46, sensitivity was 65.9% and specificity was 52.6%.

Table 12. Cut off values of PD values

PD (test results – cut off values)	**Sensitivity (%)**	**Specificity (%)**
64.6	100	0
65.9	100	0.2
69.1	90.9	0.5
73.85	79.5	4.9
75.05	70.5	6.3
76.0	68.2	8.8
76.9	61.4	12.1

77.27	59.1	13.0
78.05	56.8	14.9
79.05	54.5	17.7
80.15	47.7	20.5
81.95	43.2	30.9
82.75	40.9	35.8

The sensitivity and specificity of PD values at a cut off of 64.6 was 100% and 0% and a cut off value of 82.75, sensitivity was 40.9% and specificity was 35.8%.

Table 13. AUC values of R1, R2, PD and MyC values at different locations

Area Under the Curve

Loc - Deep (D), C-JC (C), PVWM (P), IT (I)	Test Result Variable(s)	Area	Std. Error	Asymptotic Sig.	Asymptotic 95% Confidence Interval	
					Lower Bound	Upper Bound
C	R1	.806	.072	.000	.666	.947
	R2	.833	.065	.000	.707	.960
	PD	.297	.100	.017	.101	.494
	MyC	.378	.070	.151	.240	.516
D	R1	.100	.042	.174	.017	.183
	R2	.140	.049	.221	.044	.236
	PD	.950	.031	.126	.889	1.000
	MyC	.000	.000	.089	.000	.000
I	R1	.572	.187	.591	.205	.939
	R2	.606	.158	.432	.295	.916
	PD	.399	.195	.451	.017	.780
	MyC	.507	.155	.959	.202	.812
P	R1	.694	.067	.003	.563	.825
	R2	.692	.057	.003	.579	.804
	PD	.401	.082	.125	.239	.562
	MyC	.429	.063	.275	.307	.552

The area under curve was higher for C – JC location for R1 and R2 which was not statistically significant. The AUC was lowest for deep locations except for PD values which

was also statistically not significant. The AUC values were moderate for location IT and PD had significant AUC.

Table 14. Cut off values at location C – JC for R1, R2, PD and MyC values

R1 (cut off values)	**Sensitivity (%)**	**Specificity (%)**
0.59	100	0.9
0.77	100	14.8
0.79	92.3	28.3
0.93	84.6	77.3
0.96	76.9	71.7
R2 (cut off values)	**Sensitivity (%)**	**Specificity (%)**
4.35	100	0
7.18	100	20.4
8.54	92.3	56.6
9.01	84.6	68.1
9.21	76.9	77.9
PD (cut off values)	**Sensitivity (%)**	**Specificity (%)**
68.8	100	0
70.8	92.3	0
76.0	76.9	0.9
77.27	69.2	5.3
79.0	61.5	11.5
79.15	53.8	12.4
79.75	46.2	14.2
80.45	46.2	16.8

MyC (cut off values)	Sensitivity (%)	Specificity (%)
0.15	100	4.4
0.35	100	9.7
0.95	76.9	22.1
1.05	61.5	23.0
1.15	46.2	24.8
1.65	46.2	66.4
1.85	38.5	26.3

The sensitivity and specificity of R1 values of location C – JC at a cut off of 0.59 was 100% and 0.9% and a cut off value of 0.96, sensitivity was 76.9% and specificity was 71.7%. The sensitivity and specificity of R2 values at a cut off of 4.35 was 100% and 0% and a cut off value of 9.21, sensitivity was 76.9% and specificity was 77.9%. The sensitivity and specificity of PD values at a cut off of 68.8 was 100% and 0% and a cut off value of 80.45, sensitivity was 46.2% and specificity was 16.8%. The sensitivity and specificity of MyC values at a cut off of 0.15 was 100% and 4.4% and a cut off value of 1.85, sensitivity was 38.5% and specificity was 26.3%.

Table 15. Cut off values of Deep location for R1, R2, PD and MyC values

R1 (cut off values)	Sensitivity(%)	Specificity(%)
0.58	100	2.0
0.84	100	10.0
0.86	0	10.0
R2 (cut off values)	**Sensitivity(%)**	**Specificity(%)**
2.41	100	0
7.6	100	14.0

7.71	0	14.0
PD (cut off values)	**Sensitivity(%)**	**Specificity(%)**
68.0	100	0
76.85	100	30.0
92.2	100	94.0
MyC (cut off values)	**Sensitivity(%)**	**Specificity(%)**
0.8	0	0
1.5	0	4.0

The sensitivity and specificity of R1 values of Deep location at a cut off of 0.58 was 100% and 2.0% and a cut off value of 0.86, sensitivity was 0% and specificity was 10%. The sensitivity and specificity of R2 values at a cut off of 2.41 was 100% and 0% and a cut off value of 7.71, sensitivity was 0% and specificity was 14.0%. The sensitivity and specificity of PD values at a cut off of 68.0 was 100% and 0% and a cut off value of 92.2, sensitivity was 100% and specificity was 94%. The sensitivity and specificity of MyC values at a cut off of 0.8 was 0% and 0% and a cut off value of 1.5, sensitivity was 0% and specificity was 4.0%.

Table 16. Cut off values of IT location for R1, R2, PD and MyC values

R1 (cut off values)	**Sensitivity(%)**	**Specificity(%)**
0.71	100	1.4
0.76	100	2.8
0.83	80	12.5
1.12	60	75.6
1.5	20	100
R2 (cut off values)	**Sensitivity(%)**	**Specificity(%)**
5.48	100	0

7.72	100	4.2
9.43	80	48.6
9.75	60	55.6
11.28	40	96.4
PD (cut off values)	**Sensitivity(%)**	**Specificity(%)**
64.6	100	0
67.05	100	1.4
71.35	80	4.2
74.0	60	8.3
89.8	40	86.1
MyC (cut off values)	**Sensitivity(%)**	**Specificity(%)**
0.15	100	2.8
0.85	100	19.4
1.25	80.0	19.4
2.15	60.0	27.8
5.6	40.0	50.0
16.05	40.0	90.3
17.4	20	93.1
18.45	0	93.1

The sensitivity and specificity of R1 values of IT location at a cut off of 0.71 was 100% and 1.4% and a cut off value of 1.5, sensitivity was 20% and specificity was 100%. The sensitivity and specificity of R2 values at a cut off of 5.48 was 100% and 0% and a cut off value of 11.28, sensitivity was 40% and specificity was 96.4%. The sensitivity and specificity of PD values at a cut off of 64.6 was 100% and 0% and a cut off value of 89.8, sensitivity was

40% and specificity was 86.1%. The sensitivity and specificity of MyC values at a cut off of 0.15 was 100% and 2.8% and a cut off value of 18.45, sensitivity was 0% and specificity was 93.1%.

Table 17. Cut off values of PVWM location for R1, R2, PD and MyC values

R1 (cut off values)	**Sensitivity(%)**	**Specificity(%)**
0.54	100	0.6
0.73	100	12.8
0.75	95.7	15.4
0.81	87.0	26.9
0.82	82.6	22.7
0.84	78.3	27.2
0.91	73.9	43.6
0.92	69.6	57.1
R2 (cut off values)	**Sensitivity(%)**	**Specificity(%)**
3.75	100	0
6.19	100	12.8
6.91	95.7	32.7
7.08	91.3	38.5
7.14	87.0	39.1
7.31	83.3	39.7
7.41	78.3	45.6
7.58	73.9	48.7
7.88	69.6	55.1
PD (cut off values)	**Sensitivity(%)**	**Specificity(%)**

65.2	100	0
67.15	95.7	0
71.62	87.0	0.6
73.8	82.6	2.6
75.75	69.6	5.8
76.9	65.2	8.3
78.05	60.9	9.6
79.3	56.5	14.7
80.15	52.2	16.7
82.65	47.8	30.1
84.55	43.5	42.3
89.1	39.1	73.7
MyC (cut off values)	**Sensitivity(%)**	**Specificity(%)**
0.15	91.3	3.8
0.35	87.0	12.8
0.85	73.9	23.1
1.25	65.2	33.3
1.35	60.9	35.3
1.85	47.8	45.5
2.05	43.5	47.4

The sensitivity and specificity of R1 values of PVWM location at a cut off of 0.54 was 100% and 0.6% and a cut off value of 0.92, sensitivity was 69.6% and specificity was 57.1%. The sensitivity and specificity of R2 values at a cut off of 3.75 was 100% and 0% and a cut off value of 7.88, sensitivity was 69.6% and specificity was 55.1%. The sensitivity and specificity

of PD values at a cut off of 65.2 was 100% and 0% and a cut off value of 89.1, sensitivity was 39.1% and specificity was 73.7%. The sensitivity and specificity of MyC values at a cut off of 0.15 was 91.3% and 3.8% and a cut off value of 2.05, sensitivity was 43.5% and specificity was 47.4%.

Table 18. Logistic regression for R1, R2 and PD values between non-enhancing and enhancing lesions

Variables in the Equation

		B	S.E.	Wald	df	Sig.	Exp(B)
Step 1[a]	R1	-7.743	2.361	10.754	1	.001	.000
	R2	-.019	.185	.011	1	.916	.981
	PD	-.098	.049	3.970	1	.046	.906
	Constant	18.222	5.716	10.161	1	.001	81962620.177

a. Variable(s) entered on step 1: R1, R2, PD.

R1 and PD had significantly lower odds ratio of less than 1 and R2 had non-significant odds ratio of less than 1 in this study.

Table 19. Logistic regression for R1, R2, PD and MyC values between non-enhancing and enhancing lesions

Variables in the Equation

		B	S.E.	Wald	df	Sig.	Exp(B)
Step 1[a]	R1	-16.096	3.426	22.079	1	.000	.000
	R2	.181	.232	.609	1	.435	1.199
	PD	-.057	.054	1.125	1	.289	.944
	MyC	.450	.085	28.070	1	.000	1.568
	Constant	19.233	6.495	8.769	1	.003	225421447.423

a. Variable(s) entered on step 1: R1, R2, PD, MyC.

The odd's ratio for R2 and MyC was more than 1. R1 had significant and 0 odds ratio, R2 had non-significant odds ratio of more than 1, PD had an odds ratio of less than 1 which was not significant and MyC had significant odds ratio of more than 1.

REPRESENTATIVE CASES

Case 1

26 years old female; relapsing remitting multiple sclerosis diagnosis in 2019. Currently on dimethyl fumarate since last 1 year. EDSS at last follow up 1.

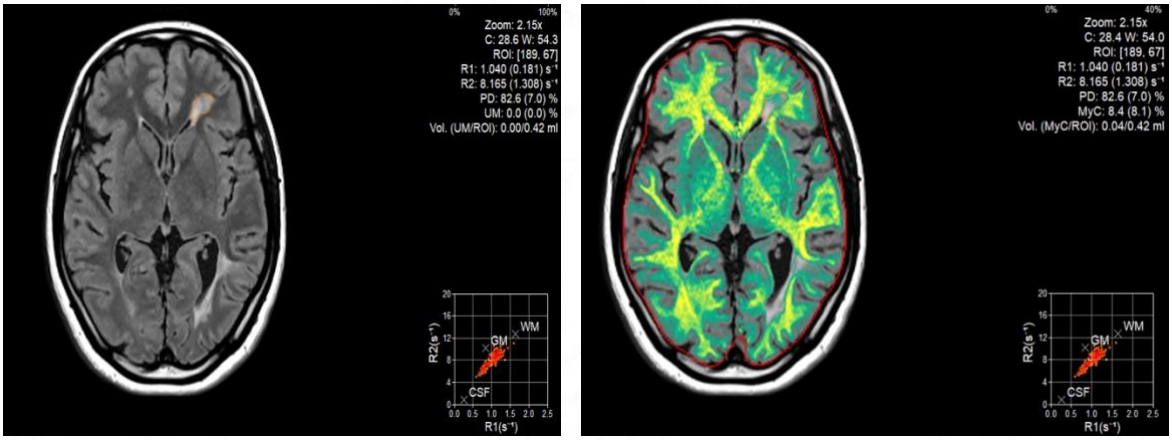

Figure 7: Synthetic FLAIR image and myelin map of patient with ROI drawn on left frontal horn periventricular white matter. Quantitative parameters for ROI are displayed on left upper corner of image.

Case 2

37 years old male; relapsing remitting multiple sclerosis diagnosis in 2002. Currently on Teriflunomide. EDSS at last follow up 2.

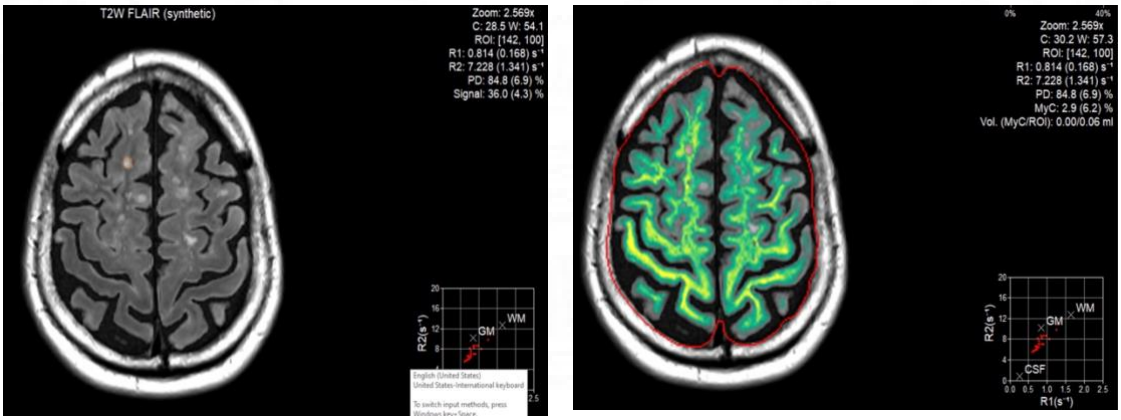

Figure 8: Synthetic FLAIR image and myelin map of patient with ROI drawn on right frontal lobe cortical-juxtacortical white matter lesion. Quantitative parameters for ROI are displayed on left upper corner of image.

Case 3

43 years old male; relapsing remitting multiple sclerosis diagnosis in 2017. Currently on dimethyl fumarate since last 3 years. EDSS at last follow up 2.

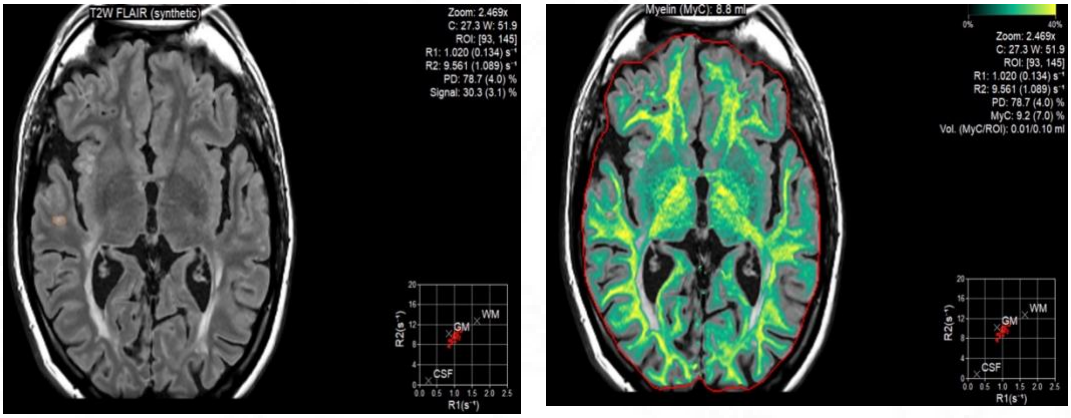

Figure 9: Synthetic FLAIR image and myelin map of patient with ROI drawn on right temporal lobe cortical-juxtacortical lesion. Quantitative parameters for ROI are displayed on left upper corner of image.

5 DISCUSSION

Multiple sclerosis is a chronic, debilitating primary demyelinating disease predominantly afflicting young adult population. Structural MRI forms the cornerstone in not only confidently diagnosing this disease entity supported by relevant clinical evaluation and application of revised McDonald's criteria (4); it also enables therapeutic monitoring and early detection of therapy related complications.

Active multiple sclerosis lesions are characterised by predominantly peri-venular inflammation without any evidence of neoangiogenesis or neovascularity (68). Blood-brain barrier breakdown is the direct consequence of this ensuing inflammation and is demonstrated on contrast enhanced MRI by intra-lesional leakage of Gadolinium contrast – appearing as nodular or less commonly, incomplete or complete ring enhancement. Enhancing multiple sclerosis lesion forms one of the defining criteria for MS diagnosis by establishing dissemination in time (4).

Due to above reasons, MS patients routinely undergo serial structural MR examinations, often with Gadolinium contrast agents to evaluate disease activity status. Routine use of Gadolinium contrast in serial imaging is not without its own set of limitations and risks. In many cases, lesional contrast enhancement may be faint or minimal due to low levels of inflammation that may go undetected. The degree of enhancement is also related to factors like time duration between contrast administration and image acquisition that has not been standardised across imaging centres, and also the contrast dosage with several studies demonstrating increased lesion detection rate with increasing doses of Gadolinium contrast (69,70). Gasperini et al (71) compared double and triple dosage of Gadolinium contrast (acquisition after 15 minutes of administration) and concluded that triple dose offered no significant benefit in improving the sensitivity of enhancing lesion detection compared to double dose of Gadolinium contrast. To complicate matters further, several studies in the last decade have highlighted the prevalence of Gadolinium deposition in deep brain structures further encouraging us to reconsider repeated contrast administration in this subset of patients (72,73). Due to all these reasons, several researchers have looked at the possibility of differentiating active from chronic MS lesions (in other words, separating active from quiescent disease) without resorting to the usage of Gadolinium contrast agents.

Sadigh et al (74) demonstrated a high concordance (95%) between contrast enhancing MS lesions and signal hyperintensity on FLAIR and double inversion recovery sequence with less than 5% enhancing lesions being missed that were either small (< 2mm) and cortical-subcortical or periventricular in location. Johnston et al (75) studied a total of 1805 MRIs performed on 920 MS patients over a period of three years and concluded that enhancing lesions are relatively uncommon on follow-up MRIs in MS patients. Further, the chances of discovering an enhancing MS lesion are minimal when 1) no enhancing lesions were noted on previous MRI and 2) no interval change in MS lesions is noted between current and previous 3D FLAIR imaging.

Shinohara et al (76) studied 93 brain conventional MR examinations and evaluated a mathematical model to predict voxel-wise enhancement and differentiate enhancing from non-enhancing plaques based on normalised T1, T2 and FLAIR-weighted signal intensities. In an interesting study by Andrada Treaba et al (77), the authors classified typical MS lesions on structural T2-weighted images into three types based on morphological parameters. Only type II lesions demonstrating T2 hyperintense centre and thin, peripheral rim of hypointensity reached diagnostic accuracy in relation to Gadolinium contrast enhancement. However, both these studies had limited accuracy, sensitivity and specificity for wider clinical application.

Recognition of the subjective variability in assessment of clinical MR imaging has shifted the focus to quantitative methods of imaging in recent times. Several MR techniques have been described enabling rapid quantification of R1 (T1 relaxation rate), R2 (T2 relaxation rate), R2* (T2* relaxation rate) and proton density (PD) in last two decades, however, most of these have been described in research arena with limited utilization in clinical setting (37–41,78–82) largely due to inhibitory long scanning duration or low SNR. In the last few years, there has been a substantial progress in development of novel quantitative MR techniques wherein, some of them can be utilized to obtain absolute quantitative values of R1, R2, PD and B1 inhomogeneity of entire imaging volume with acceptable resolution and within clinically practical scan times (83).

A few researchers have studied quantitative measurements in MS plaques with variable results. Levesque et al (84) studied the sensitivity of quantitative magnetic transfer imaging and myelin water imaging based on multicomponent T2 analysis for depicting progression of contrast enhancing MS lesions on serial MR imaging. Jurcoane et al (85) also investigated quantitative T1, PD and magnetization transfer ratio (MTR) values using conventional MR

pulse sequences and demonstrated that pre-contrast T1, PD and MTR values differed significantly between active (enhancing) and chronic (non-enhancing) lesions. However, long scan times and complex post-processing hindered its wider application.

Synthetic MRI is a novel, multi-dynamic, multi-echo pulse sequence that enables rapid and accurate quantification of R1, R2 and PD apart from providing automated, non-user dependent brain segmentation maps and myelin volume information. The scan can be performed within five minutes. Post processing is non-user dependent and takes less than 60 seconds. In current study, we observed statistically significant differences between contrast enhancing and non-enhancing MS lesion based on quantitative parameters derived from synthetic MRI. Contrast enhancing lesions had significantly higher mean R1 as well as mean R2 values and lower PD values compared to non-enhancing MS lesions. Further, normal-appearing white matter (NAWM) had even higher mean R1 and R2 values and lower mean PD values compared to contrast enhancing MS lesions. Receiver operating characteristic (ROC) curve analysis demonstrated highest AUC for mean R1 (0.667) followed by mean R2 (0.656) values in differentiating contrast enhancing from non-enhancing MS lesions. This novel technique of synthetic MRI was first used by Blystad et al (7) to compare enhancing from non-enhancing MS lesions based on quantitative parameters. They found that contrast enhancing lesions had prolonged R1 and R2 (T1 and T2 relaxation rates respectively) while PD values were lower compared to non-enhancing lesions, as noted in our study.

Literature review confirmed concordance of our findings (84,86) with a few earlier studies showing conflicting results. Larsson et al (87) observed no statistically significant difference between T1 and T2 relaxation times in acute vs chronic MS lesions; although some of these acute lesions showed elevated T1 and T2 relaxation times when imaged after 10 days. Ormerod et al (88) in their study described reduction in T1 and T2 relaxation times on sequential MR evaluation of acute MS lesions. However, in that study, acute lesions were defined by ongoing active symptomatology rather than contrast enhancement on structural MRI.

Elevated mean R2 values of contrast enhancing MS lesions as demonstrated by earlier studies and corroborated by current study has a pathophysiologic basis wherein active MS lesions are hypercellular with active macrophage and lymphocytic infiltration, presence of large reactive astrocytes along with some contribution from concurrent reactive edema (89). On the other hand, chronic inactive MS lesions are relatively hypocellular with associated

fibrillary gliosis and axonal degeneration as well as axonal loss (89). Thus, chronic MS lesions have a higher free water fraction and consequently lower mean R2 values.

It may be argued that fall in PD and raised mean R1 values in contrast enhancing lesions as noted in our study may also represent the same pathophysiologic processes of increased lesional cellularity in relation to adjacent tissue microstructure and altered free water fraction (89). However, influence of MS activity on mean R1 may be more complex since additional pathological processes like iron deposition and macrophage accumulation may also affect T1 relaxation times (85).

The receiver operating characteristic (ROC) curve analysis disclosed an AUC of 0.667 for mean R1, 0.656 for mean R2 and 0.411 for mean PD values, thereby hindering complete reliance on these objective quantitative parameters for differentiating active from chronic MS lesions. In comparison, Blystad et al (7) in their study demonstrated highest AUC of 0.832 for mean PD values for differentiating active from chronic MS lesions.

Apart from providing quantitative parametric values, synthetic MRI software can also be utilized to obtain user-independent brain tissue segmentation into gray matter, white matter, cerebrospinal fluid (CSF) as well as parametric values-based myelin maps. In the current study, we have tried to further explore the role of mean R1, R2, PD along with myelin correlated volume (MyC) values in differentiating contrast enhancing and non-enhancing MS lesions. Since myelin correlated volume (MyC) values are expected to show significant variability from one brain region to another, neuroparenchyma was further sub-divided into four compartments - periventricular white matter, deep white matter, infratentorial and cortical-juxtacortical to maintain homogeneity and comparability of myelin correlated volume (MyC) values between MS lesions.

The receiver operating characteristic (ROC) curve analysis at these four neuroparenchymal compartments revealed highest AUC for mean R1 and R2 values at cortical-juxta-cortical location – approaching 0.806 s^{-1} for mean R1 and 0.833 $^{s-1}$ for mean R2 values. However, mean myelin correlated volume (MyC) values did not yield statistically significant benefit in this compartment-wise ROC analysis at any of the four locations. This could at least partly be explained by inherently low sample size; only 24 contrast enhancing lesions were available at periventricular white matter against 177 non-enhancing lesions. These numbers are significantly lower in other compartments (14 enhancing lesions in cortical-juxtacortical

region, 1 enhancing lesion in deep white matter and 4 enhancing lesions in infratentorial region) that would have probably undermined power of the study.

MS lesions are T2 hyperintense on conventional MR imaging whereas T1 images may reveal variable signal ranging from slight to marked hypointensity (black holes). These signal alterations are likely due to demyelination, reactive edema and inflammation in varying combinations. Synthetic MRI derived myelin correlated volume (MyC) values may be more reflective of true demyelination in active MS lesion and further studies in this direction may help establish MyC as a useful marker for MS lesion evaluation.

The automated volumetric measurements available with synthetic MRI can also be used to objectively evaluate neuroparenchymal volume loss in MS patients on serial imaging as against currently performed subjective visual analysis in the clinical environment. Synthetic MRI can therefore be a valuable companion to conventional MR imaging in MS patients.

We performed synthetic MRI examination on 1.5T MR system. West et al (90) in their comparative quantitative MRI study demonstrated regional differences in brain tissue segmentation results when compared between 1.5 and 3T. As a direct consequence, synthetic MRI generated segmentation volumes may change from 1.5 to 3 or even 7T scanners and thus, cannot be extrapolated. It further stresses the fact that serial imaging should be carried out on same field strength scanner for optimal comparisons regarding neuroparenchymal atrophy.

Current study has a few limitations. Importantly, the number of contrast enhancing lesions available for analysis was relatively less and it could have indirectly affected the statistical power of the study, especially compartment-wise receiver operating characteristic (ROC) analysis. Coregistration of synthetic and conventional FLAIR images was not performed for region of interest (ROI) placement. This combined with lack of 3D synthetic imaging or even thin section synthetic FLAIR images could have led to some errors in ROI placement. This is a cross-sectional study with examined patients in various stages of disease course. Thus, MS lesions would have more pathological heterogeneity with regard to extent of demyelination, remyelination, inflammation, astrogliosis etc. This could have confounded the relaxation values especially contrast enhancing lesions, also clubbed with the fact that relaxation values in these contrast enhancing lesions vary over the course of 1-2 weeks after onset of demyelination. Preferably, the included patients should have been at an early stage that would have rendered the MS lesions under evaluation more homogeneous.

6 CONCLUSION

The current study demonstrated higher mean R1, R2 values and lower mean PD values in contrast enhancing MS lesions in comparison to non-enhancing MS lesions. Receiver operating characteristic (ROC) curve analysis revealed AUC of 0.667 and 0.656 for mean R1 and R2 values and thus had limited ability in differentiating enhancing from non-enhancing MS lesions. With user-independent brain tissue segmentation and volumetric measurements along with ability to evaluate myelin correlated volume, synthetic MRI holds significant promise in imaging evaluation of multiple sclerosis.

7 BIBLIOGRAPHY

1. Popescu BFG, Pirko I, Lucchinetti CF. Pathology of multiple sclerosis: where do we stand? Continuum (Minneap Minn). 2013 Aug;19(4 Multiple Sclerosis):901–21.
2. Hagiwara A, Kamagata K, Shimoji K, Yokoyama K, Andica C, Hori M, et al. White Matter Abnormalities in Multiple Sclerosis Evaluated by Quantitative Synthetic MRI, Diffusion Tensor Imaging, and Neurite Orientation Dispersion and Density Imaging. AJNR Am J Neuroradiol. 2019 Oct;40(10):1642–8.
3. West J, Aalto A, Tisell A, Leinhard OD, Landtblom AM, Smedby Ö, et al. Normal appearing and diffusely abnormal white matter in patients with multiple sclerosis assessed with quantitative MR. PLoS One. 2014;9(4):e95161.
4. Thompson AJ, Banwell BL, Barkhof F, Carroll WM, Coetzee T, Comi G, et al. Diagnosis of multiple sclerosis: 2017 revisions of the McDonald criteria. Lancet Neurol. 2018 Feb;17(2):162–73.
5. Sadowski EA, Bennett LK, Chan MR, Wentland AL, Garrett AL, Garrett RW, et al. Nephrogenic systemic fibrosis: risk factors and incidence estimation. Radiology. 2007 Apr;243(1):148–57.
6. Prince MR, Zhang HL, Prowda JC, Grossman ME, Silvers DN. Nephrogenic systemic fibrosis and its impact on abdominal imaging. Radiographics. 2009 Oct;29(6):1565–74.
7. Blystad I, Håkansson I, Tisell A, Ernerudh J, Smedby Ö, Lundberg P, et al. Quantitative MRI for Analysis of Active Multiple Sclerosis Lesions without Gadolinium-Based Contrast Agent. AJNR Am J Neuroradiol. 2016 Jan;37(1):94–100.
8. Warntjes JBM, Leinhard OD, West J, Lundberg P. Rapid magnetic resonance quantification on the brain: Optimization for clinical usage. Magn Reson Med. 2008 Aug;60(2):320–9.

9. Granberg T, Uppman M, Hashim F, Cananau C, Nordin LE, Shams S, et al. Clinical Feasibility of Synthetic MRI in Multiple Sclerosis: A Diagnostic and Volumetric Validation Study. AJNR Am J Neuroradiol. 2016 Jun;37(6):1023–9.

10. Vågberg M, Lindqvist T, Ambarki K, Warntjes JBM, Sundström P, Birgander R, et al. Automated determination of brain parenchymal fraction in multiple sclerosis. AJNR Am J Neuroradiol. 2013 Mar;34(3):498–504.

11. Warntjes M, Engström M, Tisell A, Lundberg P. Modeling the Presence of Myelin and Edema in the Brain Based on Multi-Parametric Quantitative MRI. Front Neurol. 2016;7:16.

12. Dobson R, Giovannoni G. Multiple sclerosis - a review. Eur J Neurol. 2019 Jan;26(1):27–40.

13. Goodin DS. The epidemiology of multiple sclerosis: insights to disease pathogenesis. Handb Clin Neurol. 2014;122:231–66.

14. Alonso A, Hernán MA. Temporal trends in the incidence of multiple sclerosis: a systematic review. Neurology. 2008 Jul 8;71(2):129–35.

15. Marrie RA, Reider N, Cohen J, Stuve O, Sorensen PS, Cutter G, et al. A systematic review of the incidence and prevalence of autoimmune disease in multiple sclerosis. Mult Scler. 2015 Mar;21(3):282–93.

16. International Multiple Sclerosis Genetics Consortium. Multiple sclerosis genomic map implicates peripheral immune cells and microglia in susceptibility. Science. 2019 Sep 27;365(6460):eaav7188.

17. De Jager PL, Jia X, Wang J, de Bakker PIW, Ottoboni L, Aggarwal NT, et al. Meta-analysis of genome scans and replication identify CD6, IRF8 and TNFRSF1A as new multiple sclerosis susceptibility loci. Nat Genet. 2009 Jul;41(7):776–82.

18. Ascherio A, Munger KL, Lennette ET, Spiegelman D, Hernán MA, Olek MJ, et al. Epstein-Barr Virus Antibodies and Risk of Multiple SclerosisA Prospective Study. JAMA. 2001 Dec 26;286(24):3083–8.

19. Wandinger K, Jabs W, Siekhaus A, Bubel S, Trillenberg P, Wagner H, et al. Association between clinical disease activity and Epstein-Barr virus reactivation in MS. Neurology. 2000 Jul 25;55(2):178–84.

20. Larsen PD, Bloomer LC, Bray PF. Epstein-Barr nuclear antigen and viral capsid antigen antibody titers in multiple sclerosis. Neurology. 1985 Mar;35(3):435–8.

21. Mokry LE, Ross S, Ahmad OS, Forgetta V, Smith GD, Goltzman D, et al. Vitamin D and Risk of Multiple Sclerosis: A Mendelian Randomization Study. PLoS Med. 2015 Aug;12(8):e1001866.

22. van der Mei I a. F, Ponsonby AL, Dwyer T, Blizzard L, Simmons R, Taylor BV, et al. Past exposure to sun, skin phenotype, and risk of multiple sclerosis: case-control study. BMJ. 2003 Aug 9;327(7410):316.

23. Lucas RM, Ponsonby AL, Dear K, Valery PC, Pender MP, Taylor BV, et al. Sun exposure and vitamin D are independent risk factors for CNS demyelination. Neurology. 2011 Feb 8;76(6):540–8.

24. Franklin GM, Nelson L. Environmental risk factors in multiple sclerosis: causes, triggers, and patient autonomy. Neurology. 2003 Oct 28;61(8):1032–4.

25. Langer-Gould A, Brara SM, Beaber BE, Koebnick C. Childhood obesity and risk of pediatric multiple sclerosis and clinically isolated syndrome. Neurology. 2013 Feb 5;80(6):548–52.

26. Bhargava P, Mowry EM. Gut microbiome and multiple sclerosis. Curr Neurol Neurosci Rep. 2014 Oct;14(10):492.

27. Dudesek A, Rimmele F, Tesar S, Kolbaske S, Rommer PS, Benecke R, et al. CLIPPERS: chronic lymphocytic inflammation with pontine perivascular enhancement responsive to steroids. Review of an increasingly recognized entity within the spectrum of inflammatory central nervous system disorders. Clin Exp Immunol. 2014 Mar;175(3):385–96.

28. Brownlee WJ, Swanton JK, Miszkiel KA, Miller DH, Ciccarelli O. Should the symptomatic region be included in dissemination in space in MRI criteria for MS? Neurology. 2016 Aug 16;87(7):680–3.

29. Kidd D, Thorpe JW, Thompson AJ, Kendall BE, Moseley IF, MacManus DG, et al. Spinal cord MRI using multi-array coils and fast spin echo. II. Findings in multiple sclerosis. Neurology. 1993 Dec;43(12):2632–7.

30. Dalton CM, Brex PA, Miszkiel KA, Fernando K, MacManus DG, Plant GT, et al. New T2 lesions enable an earlier diagnosis of multiple sclerosis in clinically isolated syndromes. Ann Neurol. 2003 May;53(5):673–6.

31. Tortorella C, Codella M, Rocca MA, Gasperini C, Capra R, Bastianello S, et al. Disease activity in multiple sclerosis studied by weekly triple-dose magnetic resonance imaging. J Neurol. 1999 Aug;246(8):689–92.

32. Smith ME, Stone LA, Albert PS, Frank JA, Martin R, Armstrong M, et al. Clinical worsening in multiple sclerosis is associated with increased frequency and area of gadopentetate dimeglumine-enhancing magnetic resonance imaging lesions. Ann Neurol. 1993 May;33(5):480–9.

33. Simon JH. From enhancing lesions to brain atrophy in relapsing MS. J Neuroimmunol. 1999 Jul 1;98(1):7–15.

34. Sajja BR, Wolinsky JS, Narayana PA. Proton magnetic resonance spectroscopy in multiple sclerosis. Neuroimaging Clin N Am. 2009 Feb;19(1):45–58.

35. Rovaris M, Filippi M. Diffusion tensor MRI in multiple sclerosis. J Neuroimaging. 2007 Apr;17 Suppl 1:27S-30S.

36. Hagiwara A, Warntjes M, Hori M, Andica C, Nakazawa M, Kumamaru KK, et al. SyMRI of the Brain: Rapid Quantification of Relaxation Rates and Proton Density, With Synthetic MRI, Automatic Brain Segmentation, and Myelin Measurement. Invest Radiol. 2017 Oct;52(10):647–57.

37. Deichmann R. Fast high-resolution T1 mapping of the human brain. Magn Reson Med. 2005 Jul;54(1):20–7.

38. Zhu DC, Penn RD. Full-brain T1 mapping through inversion recovery fast spin echo imaging with time-efficient slice ordering. Magn Reson Med. 2005 Sep;54(3):725–31.

39. Deoni SCL, Peters TM, Rutt BK. High-resolution T1 and T2 mapping of the brain in a clinically acceptable time with DESPOT1 and DESPOT2. Magn Reson Med. 2005 Jan;53(1):237–41.

40. Whittall KP, MacKay AL, Graeb DA, Nugent RA, Li DK, Paty DW. In vivo measurement of T2 distributions and water contents in normal human brain. Magn Reson Med. 1997 Jan;37(1):34–43.

41. McKenzie CA, Chen Z, Drost DJ, Prato FS. Fast acquisition of quantitative T2 maps. Magn Reson Med. 1999 Jan;41(1):208–12.

42. Pepe A, Positano V, Santarelli MF, Sorrentino F, Cracolici E, De Marchi D, et al. Multislice multiecho T2* cardiovascular magnetic resonance for detection of the heterogeneous distribution of myocardial iron overload. J Magn Reson Imaging. 2006 May;23(5):662–8.

43. Ehses P, Seiberlich N, Ma D, Breuer FA, Jakob PM, Griswold MA, et al. IR TrueFISP with a golden-ratio-based radial readout: fast quantification of T1, T2, and proton density. Magn Reson Med. 2013 Jan;69(1):71–81.

44. Ma D, Gulani V, Seiberlich N, Liu K, Sunshine JL, Duerk JL, et al. Magnetic resonance fingerprinting. Nature. 2013 Mar 14;495(7440):187–92.

45. Scheffler K, Hennig J. T(1) quantification with inversion recovery TrueFISP. Magn Reson Med. 2001 Apr;45(4):720–3.

46. Jiang Y, Ma D, Seiberlich N, Gulani V, Griswold MA. MR fingerprinting using fast imaging with steady state precession (FISP) with spiral readout. Magn Reson Med. 2015 Dec;74(6):1621–31.

47. Mehta BB, Ma D, Pierre EY, Jiang Y, Coppo S, Griswold MA. Image reconstruction algorithm for motion insensitive MR Fingerprinting (MRF): MORF. Magn Reson Med. 2018 Dec;80(6):2485–500.

48. Jiang Y, Ma D, Keenan KE, Stupic KF, Gulani V, Griswold MA. Repeatability of magnetic resonance fingerprinting T1 and T2 estimates assessed using the ISMRM/NIST MRI system phantom. Magn Reson Med. 2017 Oct;78(4):1452–7.

49. Buonincontri G, Biagi L, Retico A, Cecchi P, Cosottini M, Gallagher FA, et al. Multi-site repeatability and reproducibility of MR fingerprinting of the healthy brain at 1.5 and 3.0 T. Neuroimage. 2019 Jul 15;195:362–72.

50. Körzdörfer G, Kirsch R, Liu K, Pfeuffer J, Hensel B, Jiang Y, et al. Reproducibility and Repeatability of MR Fingerprinting Relaxometry in the Human Brain. Radiology. 2019 Aug;292(2):429–37.

51. SyntheticMR [Internet]. [cited 2022 Jul 19]. Available from: https://syntheticmr.com/resources/white-papers/

52. Ambarki K, Lindqvist T, Wåhlin A, Petterson E, Warntjes MJB, Birgander R, et al. Evaluation of automatic measurement of the intracranial volume based on quantitative MR imaging. AJNR Am J Neuroradiol. 2012 Nov;33(10):1951–6.

53. de Hoz L, Simons M. The emerging functions of oligodendrocytes in regulating neuronal network behaviour. Bioessays. 2015 Jan;37(1):60–9.

54. Duval T, Stikov N, Cohen-Adad J. Modeling white matter microstructure. Funct Neurol. 2016 Dec;31(4):217–28.

55. Heath F, Hurley SA, Johansen-Berg H, Sampaio-Baptista C. Advances in noninvasive myelin imaging. Dev Neurobiol. 2018 Feb;78(2):136–51.

56. Prasloski T, Rauscher A, MacKay AL, Hodgson M, Vavasour IM, Laule C, et al. Rapid whole cerebrum myelin water imaging using a 3D GRASE sequence. Neuroimage. 2012 Oct 15;63(1):533–9.

57. Wallaert L, Hagiwara A, Andica C, Hori M, Yamashiro K, Koshino S, et al. The Advantage of Synthetic MRI for the Visualization of Anterior Temporal Pole Lesions on Double Inversion Recovery (DIR), Phase-sensitive Inversion Recovery (PSIR), and Myelin Images in a Patient with CADASIL. Magn Reson Med Sci. 2018 Oct 10;17(4):275–6.

58. Hagiwara A, Hori M, Cohen-Adad J, Nakazawa M, Suzuki Y, Kasahara A, et al. Linearity, Bias, Intrascanner Repeatability, and Interscanner Reproducibility of Quantitative Multidynamic Multiecho Sequence for Rapid Simultaneous Relaxometry at 3 T: A Validation Study With a Standardized Phantom and Healthy Controls. Invest Radiol. 2019 Jan;54(1):39–47.

59. Andica C, Hagiwara A, Hori M, Haruyama T, Fujita S, Maekawa T, et al. Aberrant myelination in patients with Sturge-Weber syndrome analyzed using synthetic quantitative magnetic resonance imaging. Neuroradiology. 2019 Sep;61(9):1055–66.

60. Hagiwara A, Hori M, Yokoyama K, Nakazawa M, Ueda R, Horita M, et al. Analysis of White Matter Damage in Patients with Multiple Sclerosis via a Novel In Vivo MR Method

for Measuring Myelin, Axons, and G-Ratio. AJNR Am J Neuroradiol. 2017 Oct;38(10):1934–40.

61. Hagiwara A, Hori M, Suzuki M, Andica C, Nakazawa M, Tsuruta K, et al. Contrast-enhanced synthetic MRI for the detection of brain metastases. Acta Radiol Open. 2016 Feb;5(2):2058460115626757.

62. Lee EK, Lee EJ, Kim S, Lee YS. Importance of Contrast-Enhanced Fluid-Attenuated Inversion Recovery Magnetic Resonance Imaging in Various Intracranial Pathologic Conditions. Korean J Radiol. 2016 Feb;17(1):127–41.

63. Thomas-Sohl KA, Vaslow DF, Maria BL. Sturge-Weber syndrome: a review. Pediatr Neurol. 2004 May;30(5):303–10.

64. Hagiwara A, Nakazawa M, Andica C, Tsuruta K, Takano N, Hori M, et al. Dural Enhancement in a Patient with Sturge-Weber Syndrome Revealed by Double Inversion Recovery Contrast Using Synthetic MRI. Magn Reson Med Sci. 2016;15(2):151–2.

65. Virhammar J, Warntjes M, Laurell K, Larsson EM. Quantitative MRI for Rapid and User-Independent Monitoring of Intracranial CSF Volume in Hydrocephalus. AJNR Am J Neuroradiol. 2016 May;37(5):797–801.

66. Tanenbaum LN, Tsiouris AJ, Johnson AN, Naidich TP, DeLano MC, Melhem ER, et al. Synthetic MRI for Clinical Neuroimaging: Results of the Magnetic Resonance Image Compilation (MAGiC) Prospective, Multicenter, Multireader Trial. AJNR Am J Neuroradiol. 2017 Jun;38(6):1103–10.

67. Krauss W, Gunnarsson M, Nilsson M, Thunberg P. Conventional and synthetic MRI in multiple sclerosis: a comparative study. Eur Radiol. 2018 Apr;28(4):1692–700.

68. Saade C, Bou-Fakhredin R, Yousem DM, Asmar K, Naffaa L, El-Merhi F. Gadolinium and Multiple Sclerosis: Vessels, Barriers of the Brain, and Glymphatics. AJNR Am J Neuroradiol. 2018 Dec;39(12):2168–76.

69. Silver NC, Good CD, Sormani MP, MacManus DG, Thompson AJ, Filippi M, et al. A modified protocol to improve the detection of enhancing brain and spinal cord leasions in multiple sclerosis. J Neurol. 2001 Mar 1;248(3):215–24.

70. Filippi M, Yousry T, Campi A, Kandziora C, Colombo B, Voltz R, et al. Comparison of triple dose versus standard dose gadolinium-DTPA for detection of MRI enhancing lesions in patients with MS. Neurology. 1996 Feb 1;46(2):379–84.

71. Gasperini C, Paolillo A, Rovaris M, Yousry TA, Capra R, Bastianello S, et al. A comparison of the sensitivity of MRI after double- and triple-dose Gd-DTPA for detecting enhancing lesions in multiple sclerosis. Magn Reson Imaging. 2000 Jul;18(6):761–3.

72. Grahl S, Bussas M, Pongratz V, Kirschke JS, Zimmer C, Berthele A, et al. T1-Weighted Intensity Increase After a Single Administration of a Linear Gadolinium-Based Contrast Agent in Multiple Sclerosis. Clin Neuroradiol. 2021 Mar;31(1):235–43.

73. Kang H, Hii M, Le M, Tam R, Riddehough A, Traboulsee A, et al. Gadolinium Deposition in Deep Brain Structures: Relationship with Dose and Ionization of Linear Gadolinium-Based Contrast Agents. AJNR Am J Neuroradiol. 2018 Sep;39(9):1597–603.

74. Sadigh G, Saindane AM, Waldman AD, Lava NS, Hu R. Comparison of Unenhanced and Gadolinium-Enhanced Imaging in Multiple Sclerosis: Is Contrast Needed for Routine Follow-Up MRI? AJNR Am J Neuroradiol. 2019 Sep;40(9):1476–80.

75. Johnston G, Johnson T, Solomon AJ, Bazylewicz M, Allison JB, Azalone E, et al. Limited Utility of Gadolinium Contrast Administration in Routine Multiple Sclerosis Surveillance. J Neuroimaging. 2021 Jan;31(1):103–7.

76. Shinohara RT, Goldsmith J, Mateen FJ, Crainiceanu C, Reich DS. Predicting breakdown of the blood-brain barrier in multiple sclerosis without contrast agents. AJNR Am J Neuroradiol. 2012 Sep;33(8):1586–90.

77. Treabă CA, Bălaşa R, Podeanu DM, Simu IP, Buruian MM. Cerebral lesions of multiple sclerosis: is gadolinium always irreplaceable in assessing lesion activity? Diagn Interv Radiol. 2014 Apr;20(2):178–84.

78. Henderson E, McKinnon G, Lee TY, Rutt BK. A fast 3D look-locker method for volumetric T1 mapping. Magn Reson Imaging. 1999 Oct;17(8):1163–71.

79. Ordidge RJ, Gibbs P, Chapman B, Stehling MK, Mansfield P. High-speed multislice T1 mapping using inversion-recovery echo-planar imaging. Magn Reson Med. 1990 Nov;16(2):238–45.

80. Clare S, Jezzard P. Rapid T(1) mapping using multislice echo planar imaging. Magn Reson Med. 2001 Apr;45(4):630–4.

81. Neeb H, Zilles K, Shah NJ. A new method for fast quantitative mapping of absolute water content in vivo. Neuroimage. 2006 Jul 1;31(3):1156–68.

82. Kumar R, Delshad S, Woo MA, Macey PM, Harper RM. Age-related regional brain T2-relaxation changes in healthy adults. J Magn Reson Imaging. 2012 Feb;35(2):300–8.

83. Fujita S, Yokoyama K, Hagiwara A, Kato S, Andica C, Kamagata K, et al. 3D Quantitative Synthetic MRI in the Evaluation of Multiple Sclerosis Lesions. AJNR Am J Neuroradiol. 2021 Mar;42(3):471–8.

84. Levesque IR, Giacomini PS, Narayanan S, Ribeiro LT, Sled JG, Arnold DL, et al. Quantitative magnetization transfer and myelin water imaging of the evolution of acute multiple sclerosis lesions. Magn Reson Med. 2010 Mar;63(3):633–40.

85. Jurcoane A, Wagner M, Schmidt C, Mayer C, Gracien RM, Hirschmann M, et al. Within-lesion differences in quantitative MRI parameters predict contrast enhancement in multiple sclerosis. J Magn Reson Imaging. 2013 Dec;38(6):1454–61.

86. Papanikolaou N, Papadaki E, Karampekios S, Spilioti M, Maris T, Prassopoulos P, et al. T2 relaxation time analysis in patients with multiple sclerosis: correlation with magnetization transfer ratio. Eur Radiol. 2004 Jan 1;14(1):115–22.

87. Larsson HBW, Frederiksen J, Petersen J, Nordenbo A, Zeeberg I, Henriksen O, et al. Assessment of demyelination, edema, and gliosis by in vivo determination of T1 and T2 in the brain of patients with acute attack of multiple sclerosis. Magnetic Resonance in Medicine. 1989;11(3):337–48.

88. Ormerod IE, Bronstein A, Rudge P, Johnson G, Macmanus D, Halliday AM, et al. Magnetic resonance imaging in clinically isolated lesions of the brain stem. Journal of Neurology, Neurosurgery & Psychiatry. 1986 Jul 1;49(7):737–43.

89. Filippi M, Rocca MA, Barkhof F, Brück W, Chen JT, Comi G, et al. Association between pathological and MRI findings in multiple sclerosis. The Lancet Neurology. 2012 Apr 1;11(4):349–60.

90. West J, Blystad I, Engström M, Warntjes JBM, Lundberg P. Application of Quantitative MRI for Brain Tissue Segmentation at 1.5 T and 3.0 T Field Strengths. PLOS ONE. 2013 Sep 16;8(9):e74795.

PROFORMA

TITLE: Evaluating the role of synthetic MRI in differentiating active and chronic MS plaques on the basis of quantitative parameters namely R1, R2, PD and myelin water fraction.

1. Identification data

1. Unique ID number: _____

2. Serial number: _____

3. Address: _____

_____

_____

1.4 Phone number : _____

1.5 Date of registration: _____

1.6 Date of MRI study: _____

2. Demographic data

2.1 Age: _____ years

2.2 Sex: _____ 1. Male 2. Female

2.3 Occupation: _____

2.4 Education status: _____

3. Clinical presentation (1 = Yes, 0 = No)

3.1 Year and month of disease onset _____

3.2 Age at disease onset _____

3.3 Site of localization at onset _____

(1=optic nerve, 2= spinal cord, 3=cerebellar, 4=brainstem, 5= hemispheric, 6=others)

3.4 Number of clinical episodes since onset to date _____

3.4.1 Number of relapses in the last 2 years _____

3.5 On disease modifying therapy _____

3.5.1 If yes, dose and duration _____

3.6 Month and year of last relapse _____

3.7 Whether received steroid during the relapse _____

3.7.1 If yes, dose and duration _____

4. Clinical examination

4.1 Functional scores _____

4.1.1 Visual score _____

4.1.2 Brainstem score _____

4.1.3 Pyramidal score _____

4.1.4 Cerebellar score _____

4.1.5 Sensory score _____

4.1.6 Bladder/bowel score _____

4.1.7 Cognitive score _____

4.1.8 Ambulation _____

4.2 EDSS _____

श्री चित्रा तिरुनाल आयुर्विज्ञान और प्रौद्योगिकी संस्थान, त्रिवेंद्रम - 695 011, केरल, भारत
SREE CHITRA TIRUNAL INSTITUTE FOR MEDICAL SCIENCES AND TECHNOLOGY
TRIVANDRUM - 695 011, KERALA, INDIA
(एक राष्ट्रीय महत्व का संस्थान, विज्ञान एवं प्रौद्योगिकी विभाग, भारत सरकार)
(An Institution of National Importance, Department of Science and Technology, Government of India)
टेलीफॉन नं./Telephone No.: 0471-2443152 फैक्स/Fax: 0471-2446433, 2550728
ई-मेल/E-mail: sct@sctimst.ac.in वेबसाइट/Website: www.sctimst.ac.in

Institutional Ethics Committee

(IEC Regn No. ECR/189/Inst/KL/2013/RR-16)

SCT/IEC/1620/DECEMBER-2020 16.12.2020

Dr Sachin Girdhar
Senior Resident
Dept of IS & IR, SCTIMST

Dear Dr Sachin Girdhar,

Thank you for submitting documents related to your proposal titled "**EVALUATING THE ROLE OF SYNTHETIC MAGNETIC RESONANCE IMAGING (MRI) IN DIFFERENTIATING ACTIVE AND CHRONIC MULTIPLE SCLEROSIS (MS) PLAQUES ON THE BASIS OF QUANTITATIVE PARAMETERS NAMELY T1 RELAXATION RATE (R1), T2 RELAXATION RATE (R2), PROTON DENSITY (PD) AND MYELIN WATER FRACTION (MWF)** (IEC/1620)" to the IEC for review.

The following documents were reviewed:

1. Full proposal
2. IEC Application Form
3. Covering letter addressed to the Chairman, IEC, SCTIMST dated 22.10.2020 forwarded by HOD
4. TAC Approval Letter
5. Information Sheet in English
6. Information Sheet in Malayalam
7. Consent Form in English
8. Consent Form in Malayalam
9. CV of Dr Sachin Girdhar with MCI registration number
10. CV of Dr Bejoy Thomas with TCMC registration number
11. CV of Dr Aniruddha PR with KMC registration number '
12. CV of Dr C Kesavadas with TCMC registration number
13. CV of Dr Sruthi S Nair with TCMC registration number
14. Covering letter addressed to the Chairman, IEC, SCTIMST dated 24.10.2020
15. Checklist

The following members of the Students Sub-Committee of the Institutional Ethics Committee participated in the discussions held on Dec 9, 2020 at the offices and residences of the members

SL. No.	Member Name	Highest Degree	Gender	Scientific /Non Scientific	Affiliation with Institution(s)
1.	Dr. R V G Menon	M Tech, PhD	Male	Lay Person (Chairman)	No
2.	Dr. Harikrishnan S	MD, DM (Cardiology) DNB (Cardiology)	Male	Clinician	Yes
3.	Dr. Kala Kesavan. P	MBBS, MD	Female	Basic Medical Scientist	No
4.	Dr. Rema M. N	MD	Female	Basic Medical Scientist	No
5.	Dr. Christina George	MD Psychiatry	Female	Clinician	No
6.	Dr. Mala Ramanathan	PhD	Female	Social Scientist (Member Secretary)	Yes

IEC Decision
The IEC approved the conduct of the study in the present form.

Remarks:
The Institutional Ethics Committee expects to be informed about the progress of the study, any SAE occurring in the course of the study, any changes in the protocol and patient information/informed consent and asks to be provided a copy of the final report.

There was no member of the study team who participated in voting / decision making process. The ethics committee is organized and operated according to the requirements of Good Clinical Practice and the requirements of the Indian Council of Medical Research (ICMR).

Sincerely,

Mala Ramanathan
Member Secretary, IEC

RE-2022-39540-plag-report

ORIGINALITY REPORT

9%	6%	7%	2%
SIMILARITY INDEX	INTERNET SOURCES	PUBLICATIONS	STUDENT PAPERS

PRIMARY SOURCES

1	Ida Blystad. "Clinical Applications of Synthetic MRI of the Brain", Linkoping University Electronic Press, 2017 Publication	1%
2	Blystad, I., I. Hakansson, A. Tisell, J. Ernerudh, O. Smedby, P. Lundberg, and E.- M. Larsson. "Quantitative MRI for Analysis of Active Multiple Sclerosis Lesions without Gadolinium-Based Contrast Agent", American Journal of Neuroradiology, 2015. Publication	<1%
3	Submitted to University of Strathclyde Student Paper	<1%
4	clinical.netforum.healthcare.philips.com Internet Source	<1%
5	www.ncbi.nlm.nih.gov Internet Source	<1%
6	www.science.gov Internet Source	<1%

7	"ECR 2020 Book of Abstracts", Insights into Imaging, 2020 Publication	<1 %
8	epublications.uef.fi Internet Source	<1 %
9	www.mdpi.com Internet Source	<1 %
10	Submitted to University of Cumbria Student Paper	<1 %
11	Chun-Chi Chou, Shu-Yi Wei, Yuan-Chao Lou, Chinpan Chen. "In-depth study of DNA binding of Cys2His2 finger domains in testis zinc-finger protein", PLOS ONE, 2017 Publication	<1 %
12	"Poster Session 1", Multiple Sclerosis Journal, 2015 Publication	<1 %
13	assets.researchsquare.com Internet Source	<1 %
14	www.ajnr.org Internet Source	<1 %
15	academic.oup.com Internet Source	<1 %
16	ejrnm.springeropen.com Internet Source	<1 %

17	hdl.handle.net Internet Source	<1 %
18	tcr.amegroups.com Internet Source	<1 %
19	Alina Jurcoane, Marlies Wagner, Christoph Schmidt, Christoph Mayer et al. "Within-lesion differences in quantitative MRI parameters predict contrast enhancement in multiple sclerosis", Journal of Magnetic Resonance Imaging, 2013 Publication	<1 %
20	Submitted to Monash University Student Paper	<1 %
21	archive.org Internet Source	<1 %
22	id.booksc.org Internet Source	<1 %
23	Submitted to Cardiff University Student Paper	<1 %
24	Submitted to October University for Modern Sciences and Arts (MSA) Student Paper	<1 %
25	core.ac.uk Internet Source	<1 %

26	"Scientific Sessions", European Radiology Supplements, 2008 Publication	<1 %
27	"Twentieth Meeting of the European Neurological Society 19–23 June 2010 Berlin, Germany", Journal of Neurology, 2010 Publication	<1 %
28	Wolf-Dieter Zech, Nicole Schwendener, Anders Persson, Marcel J. Warntjes, Christian Jackowski. "Postmortem MR quantification of the heart for characterization and differentiation of ischaemic myocardial lesions", European Radiology, 2015 Publication	<1 %
29	coek.info Internet Source	<1 %
30	"Therapeutic Decision Making in Multiple Sclerosis: Best Practice Algorithms for the MS Care Clinician", International Journal of MS Care, 2014 Publication	<1 %
31	Submitted to University of Lincoln Student Paper	<1 %
32	centogene.azureedge.net Internet Source	<1 %
33	link.springer.com Internet Source	<1 %

34	managementjournal.usamv.ro Internet Source	<1%
35	n.neurology.org Internet Source	<1%
36	Megumi Matsuda, Takaharu Tsuda, Rui Ebihara, Wataru Toshimori et al. " Enhanced Masses on Contrast - Enhanced Breast: Differentiation Using a Combination of Dynamic Contrast - Enhanced and Quantitative Evaluation with Synthetic ", Journal of Magnetic Resonance Imaging, 2020 Publication	<1%
37	www.karger.com Internet Source	<1%
38	Kelvin K. Leung, Ian M. Malone, Sebastien Ourselin, Jeffrey L. Gunter et al. "Effects of changing from non-accelerated to accelerated MRI for follow-up in brain atrophy measurement", NeuroImage, 2015 Publication	<1%
39	Massimo Filippi, Maria A. Rocca. "MR Imaging of Multiple Sclerosis", Radiology, 2011 Publication	<1%
40	repository-tnmgrmu.ac.in Internet Source	<1%
41	www.tdx.cat	

	Internet Source	<1%
42	en.wikipedia.org Internet Source	<1%
43	entokey.com Internet Source	<1%
44	globalheartjournal.com Internet Source	<1%
45	scielo.conicyt.cl Internet Source	<1%
46	www.hindawi.com Internet Source	<1%
47	"Abstracts", Multiple Sclerosis, 03/01/2007 Publication	<1%
48	"Poster I", Multiple Sclerosis Journal, 2012 Publication	<1%
49	M. Drake-Pérez, B.M.A. Delattre, J. Boto, A. Fitsiori, K.-O. Lovblad, S. Boudabbous, M.I. Vargas. "Normal Values of Magnetic Relaxation Parameters of Spine Components with the Synthetic MRI Sequence", American Journal of Neuroradiology, 2018 Publication	<1%
50	S M Leary. "Multiple sclerosis: diagnosis and the management of acute relapses",	<1%

Postgraduate Medical Journal, 2005
Publication

51	Sharon Portnoy, Mark Osmond, Meng Yuan Zhu, Mike Seed, John G. Sled, Christopher K. Macgowan. "Relaxation properties of human umbilical cord blood at 1.5 Tesla", Magnetic Resonance in Medicine, 2017 Publication	<1 %
52	Wolfgang Krauss, Martin Gunnarsson, Torbjörn Andersson, Per Thunberg. "Accuracy and reproducibility of a quantitative magnetic resonance imaging method for concurrent measurements of tissue relaxation times and proton density", Magnetic Resonance Imaging, 2015 Publication	<1 %
53	arxiv.org Internet Source	<1 %
54	careersdocbox.com Internet Source	<1 %
55	ejournal.unib.ac.id Internet Source	<1 %
56	Alan J Thompson, Brenda L Banwell, Frederik Barkhof, William M Carroll et al. "Diagnosis of multiple sclerosis: 2017 revisions of the McDonald criteria", The Lancet Neurology, 2018 Publication	<1 %

57	"37th EUROPEAN SOCIETY OF NEURORADIOLOGY ANNUAL MEETING, September 28 – October 1, 2013", Neuroradiology, 2013 Publication	<1%
58	"Poster II", Multiple Sclerosis Journal, 2012. Publication	<1%
59	Sand, Ilana Katz. "Classification, diagnosis, and differential diagnosis of multiple sclerosis :", Current Opinion in Neurology, 2015. Publication	<1%

Exclude quotes	On	Exclude matches	Off
Exclude bibliography	On		